



AD627138



EXPERIMENTAL STUDY OF STATIC AND DYNAMIC FRICTION BETWEEN SOIL AND TYPICAL CONSTRUCTION MATERIALS

G. A. Leonards
Purdue University
School of Civil Engineering
Lafayette, Indiana

CLEARING CHARGE	
FOR FEDERAL GOVERNMENT	
TECHNICAL REPORT	
Hardcopy	Microfilm
\$3.00	\$0.75 76 us
ARCHIVE COPY	
<i>Code 1</i>	

TECHNICAL REPORT NO. AFWL-TR-65-161

December 1965

PROCESSING COPY

AIR FORCE WEAPONS LABORATORY
Research and Technology Division
Air Force Systems Command
Kirtland Air Force Base
New Mexico



ACCESSION NO.		
CFSTI		
DDC		
ENR.		
JUSTIFIED		
BY		
DISTRIBUTION STATEMENT		
DIST. AVAIL. AND CONTROL		

Research and Technology Division
 AIR FORCE WEAPONS LABORATORY
 Air Force Systems Command
 Kirtland Air Force Base
 New Mexico

When U. S. Government drawings, specifications, or other data are used for any purpose other than a definitely related Government procurement operation, the Government thereby incurs no responsibility nor any obligation whatsoever, and the fact that the Government may have formulated, furnished, or in any way supplied the said drawings, specifications, or other data, is not to be regarded by implication or otherwise, as in any manner licensing the holder or any other person or corporation, or conveying any rights or permission to manufacture, use, or sell any patented invention that may in any way be related thereto.

This report is made available for study with the understanding that proprietary interests in and relating thereto will not be impaired. In case of apparent conflict or any other questions between the Government's rights and those of others, notify the Judge Advocate, Air Force Systems Command, Andrews Air Force Base, Washington, D. C. 20331.

Distribution of this document is unlimited.

EXPERIMENTAL STUDY OF STATIC AND DYNAMIC
FRICTION BETWEEN SOIL AND TYPICAL CONSTRUCTION MATERIALS

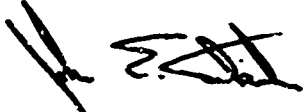
G. A. Leonards
Purdue University
School of Civil Engineering
Lafayette, Indiana

Distribution of this document
is unlimited.

FOREWORD

This report was prepared by the School of Engineering, Purdue University, Lafayette, Indiana, under contract AF 29(601)-5204. The research was performed under Program Element 7.60.06.01.D, Project 5710, Subtask 13.144, and was funded by the Defense Atomic Support Agency (DASA).

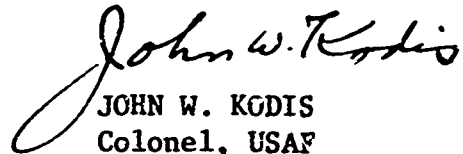
Inclusive dates of research were 1 April 1962 to 1 April 1965. The report was submitted 24 November 1965 by the Air Force Weapons Laboratory project officer 1Lt John E. Seknicka (WLDC).



JOHN E. SEKNICKA
1Lt, USAF
Project Officer



ROBERT E. CRAWFORD
Major, USAF
Deputy Chief, Civil Engineering
Branch



JOHN W. KODIS
Colonel, USAF
Chief, Development Division

ABSTRACT

A report is made of research carried out at Purdue University to determine, on the basis of laboratory measurements, the coefficient of friction between two sands of different gradation (one with angular and the other with rounded particles) in contact with Portland cement mortar, steel, teflon, and graphite. In the static tests, loads were applied at a uniform rate until slip occurred in approximately 5 minutes. Dynamic loads were applied by means of a shock tube, which produced a step-like forcing function; slip usually occurred in approximately 2 milliseconds or less. It was found that the coefficients of friction depend on the relative size, shape and surface roughness of the sand grains with respect to that of the surface in question; when the sliding surface is "rough" in comparison with the sand particles, the coefficient of friction approaches the coefficient of internal friction of the sand. Both graphite and teflon serve as friction reducers, compared to the plain surfaces, irrespective of the rate at which slip is initiated. For plain steel or cement mortar, the dynamic coefficient of friction was greater than the static coefficient of friction by about 25 percent, unless the static coefficient was such that sand/sand slip was approached. The angle of shearing resistance of the sand thus provides an upper limit to the coefficient of wall friction at all rates of loading.

This page intentionally left blank.

TABLE OF CONTENTS

<u>Section</u>		<u>Page</u>
I	INTRODUCTION.	1
II	EXPERIMENTAL CONCEPT.	2
	General Considerations	2
	Dynamic Friction Force	4
	Inertia Force.	6
	Dynamic Normal Force	6
III	MATERIALS	7
	Sand	7
	Test Rods.	9
IV	APPARATUS AND PROCEDURES.	15
	Sample Preparation	15
	Static Tests	23
	Dynamic Tests.	25
V	RESULTS	32
	Static Friction Tests.	32
	Dynamic Tests.	40
VI	CONCLUSIONS	53
	REFERENCES.	55
	APPENDICES.	
	A: DETERMINATION OF FORCING FUNCTION.	56
	B: USE OF LINEAR VARIABLE DIFFERENTIAL TRANSFORMER FOR VELOCITY MEASUREMENTS	58
	C: SAMPLE CALCULATIONS.	62
	Static Tests.	62
	Dynamic Tests	64
	DISTRIBUTION.	66

LIST OF TABLES

<u>Table No.</u>	<u>Page</u>
I. Grain Size Distribution for 60-80 Sand	7
II. Types of Surfaces Tested	9
III. Comparison of μ_s Values for Different Types of Tests Using 20-30 Sand	33
IV. Values of μ_s Based on Static Tests with 60-80 Sand	37
V. Values of μ_s Based on Static Tests with 20-30 Sand	38
VI. Comparison of μ_s Values.	40
VII. ΔN_s for Uncapped and Capped Gages at Time of Slip.	45
VIII. Values of μ_d for 60-80 Sand on Plain Steel	46
IX. Values of μ_d for 20-30 Sand on Smooth Mortar	47
X. Values of μ_d for 20-30 Sand on Rough Mortar.	48
XI. Values of μ_d for 20-30 Sand on Teflon Coated Smooth Mortar	49
XII. Values of μ_d for 20-30 Sand on Teflon Coated Steel	50
XIII. Values of μ_d for 20-30 Sand on Graphite Coated Smooth Mortar	51
XIV. Comparison of Static and Dynamic Coefficients of Friction.	52

LIST OF FIGURES

<u>Figure No.</u>	<u>Page</u>
1. Schematic Diagram of Experimental Concept.	3
2. Forcing Functions, F(t).	5
3. Failure Conditions at Peak $\sigma_1 - \sigma_3$ in the Triaxial Test, 20-30 Sand	8
4. Failure Conditions at Peak $\sigma_1 - \sigma_3$ in the Triaxial Test, 60-80 Sand	10
5. Photomicrograph of Sands (Multiplication x 60)	11
6. Test Rods.	14
7. Mold for Sample Preparation.	16
8. Sand "Raining" Tube.	17
9A. Stress Gage and Gage Placing Tool.	19
9B. Gage Locations	20
10. Sample Headcap	20
11. Extruding the Sample from the Mold	21
12. The Extruded Sample.	22
13. Sample Housing Showing Alignment Guides and Reaction Ring.	22
14. Apparatus for Auxilliary Static Friction Tests	24
15. Proving Ring and Displacement Dial in Position for Static Tests	26
16. Piston Assembly.	27
17. LVDT Mounting.	27
18. Dynamic Test Assembly.	28
19. Detail of Headcap.	28

LIST OF FIGURES (continued)

<u>Figure No.</u>	<u>Page</u>
20. General View of Dynamic Test Set-Up.	29
21. Capped Stress Gage	31
22. Force vs. Displacement (60-80 sand on plain smooth mortar) Static Test No. 7.	34
23. Force vs. Displacement (20-30 sand on plain rough mortar) Static Test No. 14	35
24. Force vs. Displacement (20-30 sand on Teflon coated steel) Static Test No. 15	36
25. Typical LVDT Trace	41
26. Typical Pressure Gage Trace.	41
27. ΔN_s vs. Station Along Rod (at slip).	43
28. Verification Curves for F(t)	57
29. Circuit Diagram for LVDT Used as a Velocity Transducer . .	59
30. Typical Trace for Velometer Calibration.	60
31. Vacuum Gage Calibration.	63

SECTION I
INTRODUCTION

The work reported herein was carried out under contract AF29 (601)-5204, "Experimental Study of Soil-Wall Shear," an integral part of a large-scale research program on protective construction sponsored by the United States Air Force. In connection with the design of such structures, questions arise relating to how much shear can be transferred from the soil to the structure before slip will occur; namely, if the stresses are transmitted as shock waves, is the coefficient of friction much greater than under conditions where they are gradually applied? What types of lubricants can effectively reduce the magnitude of the transmitted shear stresses? Since practically nothing was known concerning the dynamic friction of soil sliding on other materials, the objective of the study was limited to a preliminary investigation -- simple in concept and capable of rapid execution -- that could provide reliable answers to the questions raised.

This document constitutes the final report of the laboratory studies conducted during the period 1 April 1962 through 1 April 1965 to fulfill the stated objective. The project was carried out under the direction of G. A. Leonards and M. E. Harr. Major John T. Gaffey, II, developed the instrumentation and obtained initial data on the static and dynamic friction coefficients on one sand for his PhD dissertation (1)*. William F. Brumund refined the experimental techniques and completed the study (including tests on two sands) for his M.S.C.E. thesis (2). The report was prepared by G. A. Leonards.

* Numbers in parentheses refer to the References on page 55.

SECTION II

EXPERIMENTAL CONCEPT

1. GENERAL CONSIDERATIONS

The shearing force, F , required to initiate slip of one body on another divided by the normal force, N , between the contact surfaces is called the coefficient of friction, μ .

The coefficient of friction between sands and such construction materials as steel and concrete (including the effects of friction reducing liners) was measured to compare values of μ obtained when slip is initiated by a slowly applied friction force (in about five minutes) as opposed to one applied very rapidly (in one millisecond or less), hereafter referred to as "static" and "dynamic" tests, respectively.

The test set-up chosen for the study is shown schematically in Figure 1 (mechanical details are described under "Apparatus and Procedures"). It consisted of a cylinder of sand encased in a rubber membrane with a rod located on its axis. By evacuating the air from the inside of the membrane a normal pressure was applied on the sand/rod interface. The rod was then caused to slip relative to the sand by the application of "static" or "dynamic" forces in an axial direction.

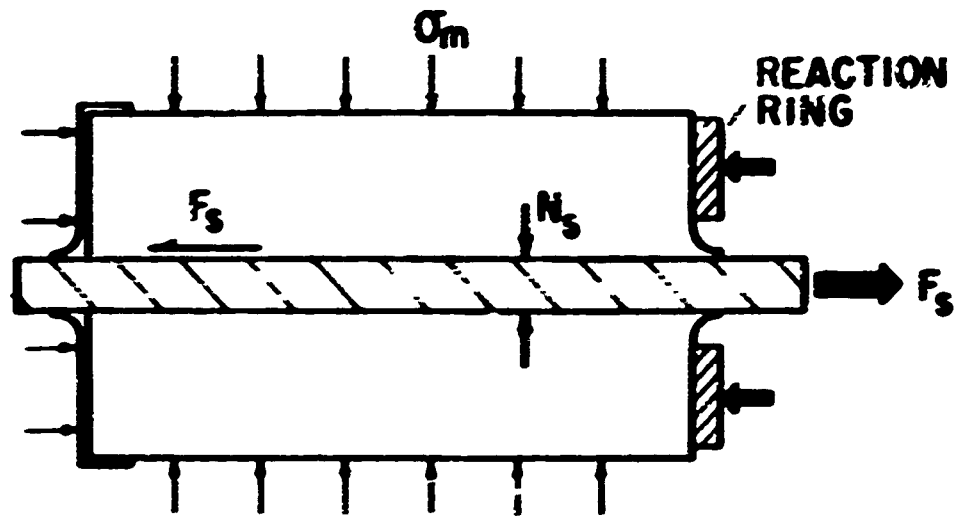
To determine the coefficient of static friction, μ_s , defined as:

$$\mu_s = \frac{F_s}{N_s} \quad (1)$$

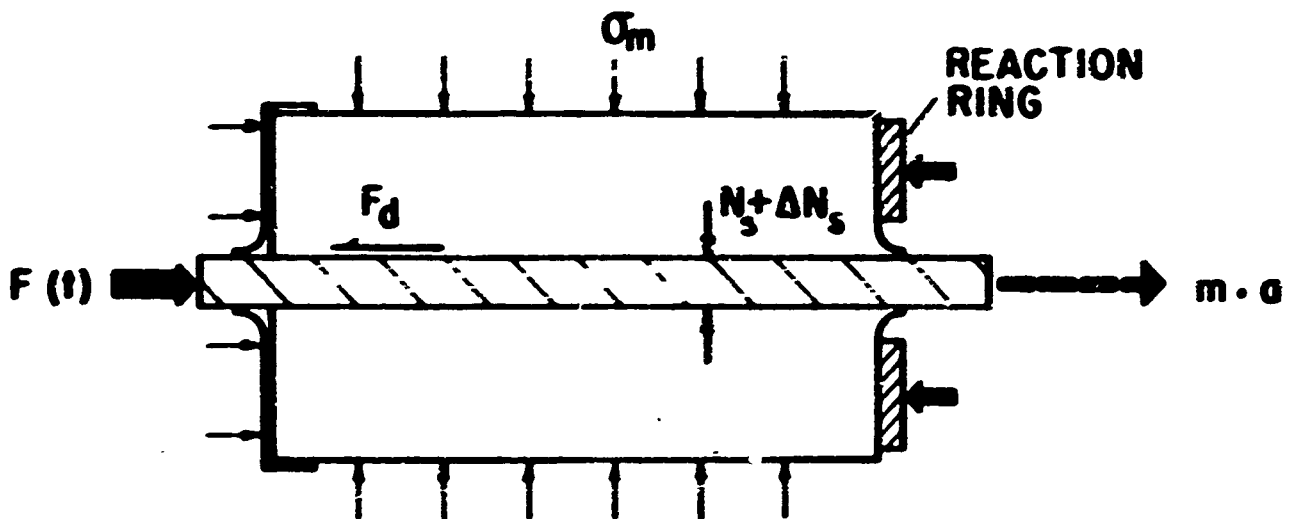
where

F_s = static friction force on the slip surface, at slip

N_s = static normal force applied on the surface, at slip



a. THE STATIC MODEL



b. THE DYNAMIC MODEL

FIG. 1 SCHEMATIC DIAGRAM OF EXPERIMENTAL CONCEPT

F_s was measured directly by weighing the quantity of water added to the loading frame when slip was induced. N_s was obtained indirectly; auxiliary tests to be described later showed that N_s was equal to the confining pressure (σ_m) due to the vacuum, times the area of the sand/rod interface. The confining pressure was measured directly with a bourdon gage.

To determine the coefficient of dynamic friction, μ_d , defined as:

$$\mu_d = \frac{F_d}{N_d} = \frac{F(t) - ma}{N_s + \Delta N_s} \quad (2)$$

where

F_d = dynamic friction force

N_d = dynamic normal force

$F(t)$ = the applied forcing function

m = total mass of moving system

a = acceleration of the moving system

N_s = static normal force

ΔN_s = change in static normal force due to application of the dynamic force

The terms on the right hand side of equation 2 (other than N_s) were obtained by direct measurement. Miscellaneous friction forces in the apparatus were also measured and found to be negligible (1).

2. DYNAMIC FRICTION FORCE

A shock tube, fitted with a piston assembly, transmitted a forcing function to the test rod. Figure 2 shows the variation in forcing functions with time for various initial pressures in the shock tube. Details for determining the forcing functions may be found in Appendix A.

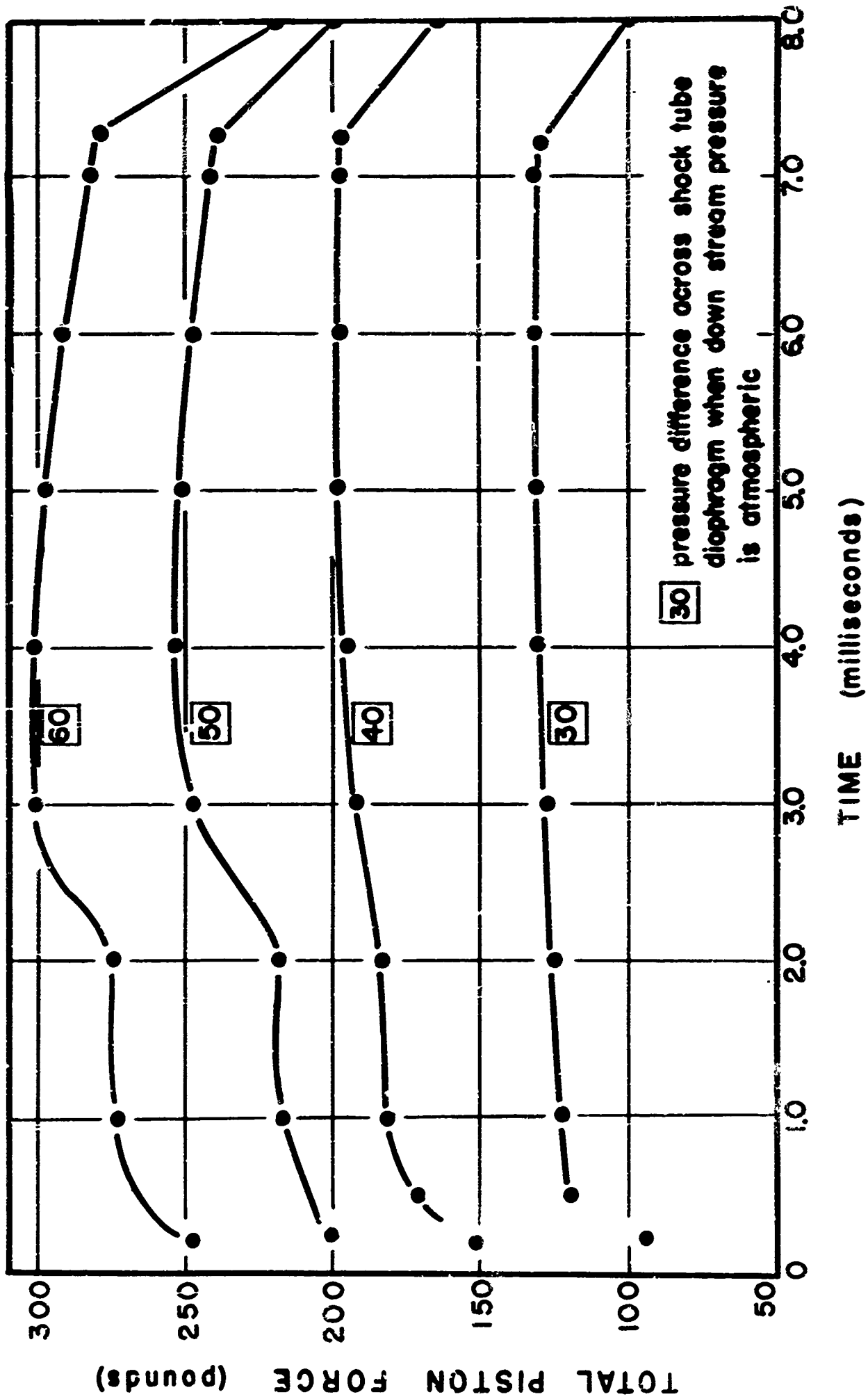


FIG. 2 FORCING FUNCTIONS, $F(t)$

3. INERTIA FORCE

To determine the inertia forces, use was made of a linear variable differential transformer (LVDT). The LVDT, utilizing single sweep oscilloscope photography, was calibrated to display a trace of the rod velocity with time. As the slope of the velocity-time curve equals the acceleration, the inertial correction could be made. The procedures used to calibrate the LVDT for use as a velocity meter are given in Appendix B.

4. DYNAMIC NORMAL FORCE

Initially it was thought that during application of the dynamic shearing force the normal force on the sand/rod interface might change. Accordingly, it was decided to measure the change in static normal force using piezoelectric stress gages similar to those designed for another study (3).

SECTION III

MATERIALS

1. SAND

Two types of sand were used. One type was a uniformly graded quartz sand, hereafter called "20-30" sand, 100 percent of which passed the #20 and was retained on the #30 U.S. standard sieve. The specific gravity of the solids of this sand was found to be 2.65. The "raining" technique for sand placement resulted in a void ratio of 0.49, or an (air) dry density of about 110 pounds per cubic foot, which corresponds to a relative density of about 92 percent. Constant strain rate, vacuum triaxial tests give an angle of shearing resistance, $\phi' = 40^\circ$ (Figure 3).

The other sand used was a crushed quartz sand, hereafter referred to as "60-80" sand, because 70 percent of the particles was retained between the #60 and #80 U.S. standard sieves. Table I gives the grain size distribution of this sand.

TABLE I
GRAIN SIZE DISTRIBUTION FOR 60-80 SAND

<u>U.S. Sieve</u>	<u>% Pass:</u>
# 40	100
# 60	75.6
# 80	7.0
#100	0.6

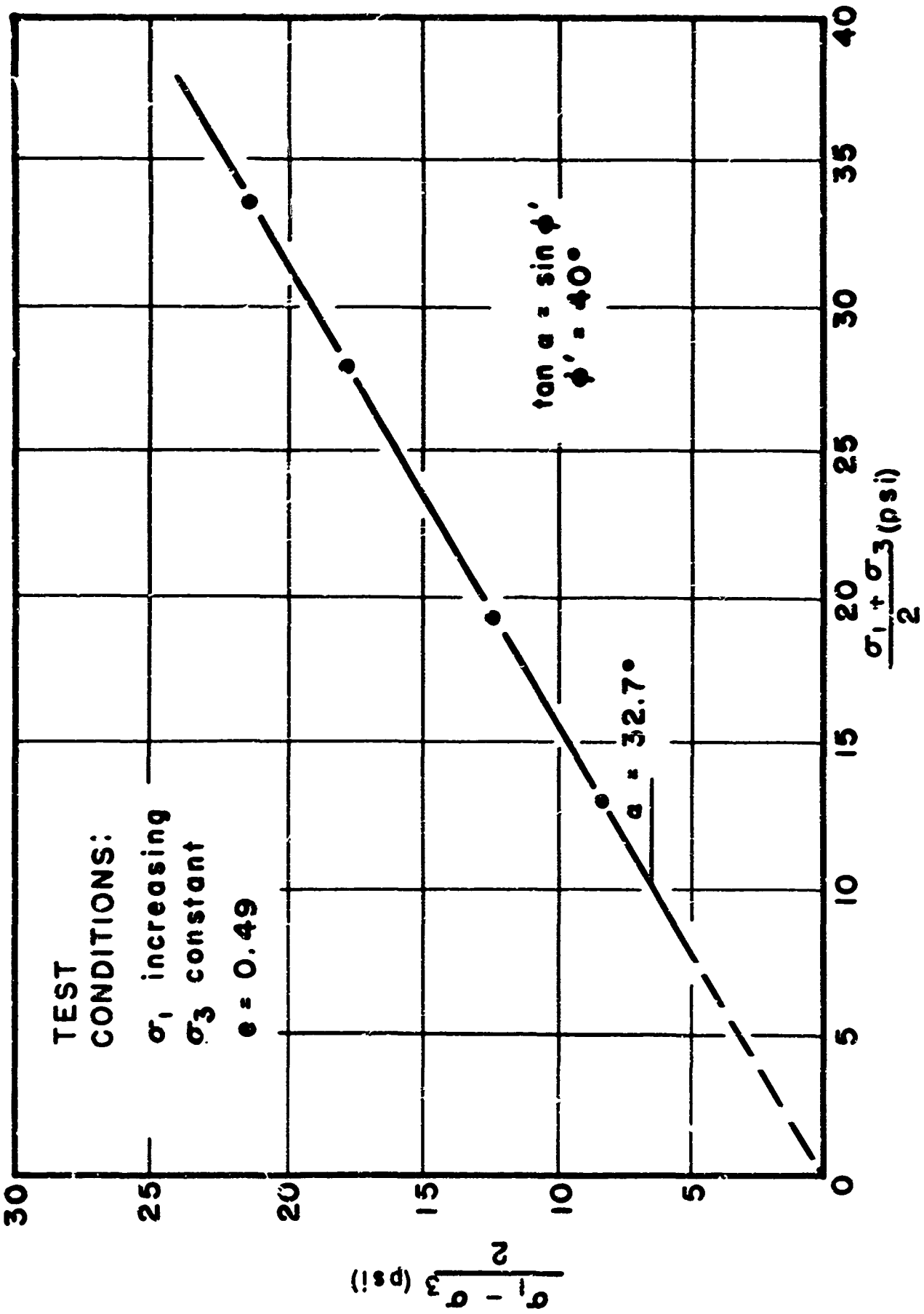


FIG. 3 FAILURE CONDITIONS AT PEAK $\sigma_1 - \sigma_3$ IN THE TRIAXIAL TEST FOR 20 - 30 SAND

The specific gravity of solids was found to be 2.66. The "raining" method of sand placement resulted in a void ratio of 0.75, or an (air) dry density of about 95 pounds per cubic foot, which corresponds to a relative density of approximately 90 percent. Constant strain rate, vacuum triaxial tests gave an angle of shearing resistance $\phi' = 48^\circ$ (Figure 4).

Because the 60-80 sand was crushed, the particles were very angular. The 20-30 sand particles were, for the most part, rounded. Figure 5 shows a photomicrograph of the two sands at the same magnification (60 x). These differences in size, angularity and surface texture of the grains affected the test results significantly.

2. TEST RODS

Three types of rods were used: polished steel, smooth mortar, and rough mortar. Graphite and teflon were applied to some of the test rods to act as friction reducers. The various surfaces that were tested are listed in Table II.

TABLE II
TYPES OF SURFACES TESTED

1. Plain Steel (square)
2. Teflon coated Steel (square)
3. Graphite coated Steel (square)
4. Plain smooth Mortar (round)
5. Teflon coated smooth Mortar (round)
6. Graphite coated smooth Mortar (round)
7. Plain rough Mortar (round)

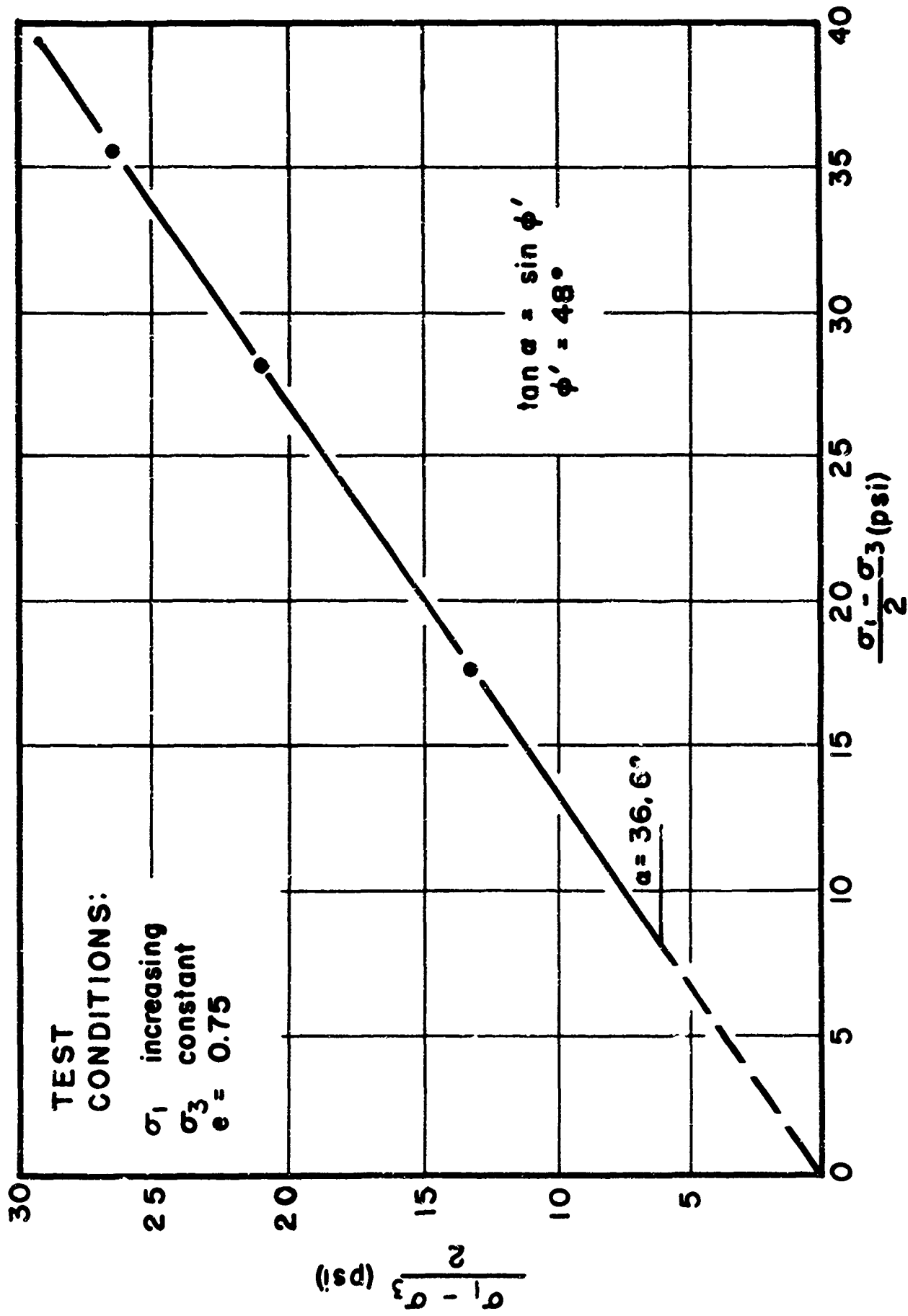


FIG. 4 FAILURE CONDITIONS AT PEAK $\sigma_1 - \sigma_3$ IN THE TRIAXIAL TEST FOR 60 - 80 SAND



(b) 20-30 Sand



(a) 60-80 Sand

FIG. 5. PHOTOMICROGRAPH OF SANDS (Multiplication x 60)

The steel test rod used was machined from a mild (low carbon) steel bar finished with a very fine emery cloth, which produced a smooth test surface. The rod was square, each side being $1/8$ inches wide, and 10 inches long. In order for the rod to slip freely through the circular orifice in the membrane, each end was turned down to a $1\ 1/8$ inch diameter cylinder, and a $1/2$ inch threaded extension was provided to facilitate connecting the static pull apparatus or the piston assembly for the dynamic test. The total length of the steel rod was 15 inches.

A graphite coating was applied to the steel surface with a soft pencil and Dixon No. 2 graphite flakes. The surface of the rod was first rubbed thoroughly with the pencil; then graphite flakes were rubbed on with a cotton applicator.

A Teflon coating was applied to the steel surface by covering the rod with $1/2$ -inch wide by 0.006-inch thick Teflon "Temp-R-Tape." Two layers of tape were applied to the rod, care being taken so that no two of the longitudinal butted joints occurred in the same place.

Preliminary tests indicated that concrete rods $1\ 1/8$ and 2 inches in diameter by 15 inches long would "fit" the combination of forces available from the shock tube and the expected friction forces. To provide for possible extensions to the study, the aggregate used was chosen for its availability and reproducibility of size, surface texture, and shape. Accordingly, it was decided to use the 20-30 sand (ASTM designation C190-59) as a one-sized aggregate. Type III (high early strength) Portland cement, conforming to ASTM Designation C150-61, was used in the following proportions:

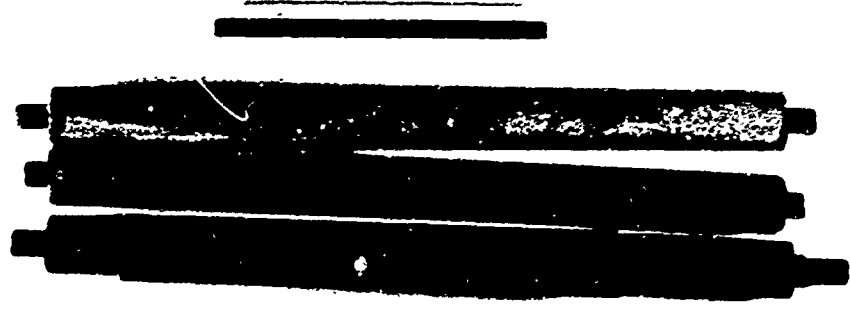
Water-cement ratio (by weight), 0.45.

Aggregate-cement ratio (by weight), 0.45.

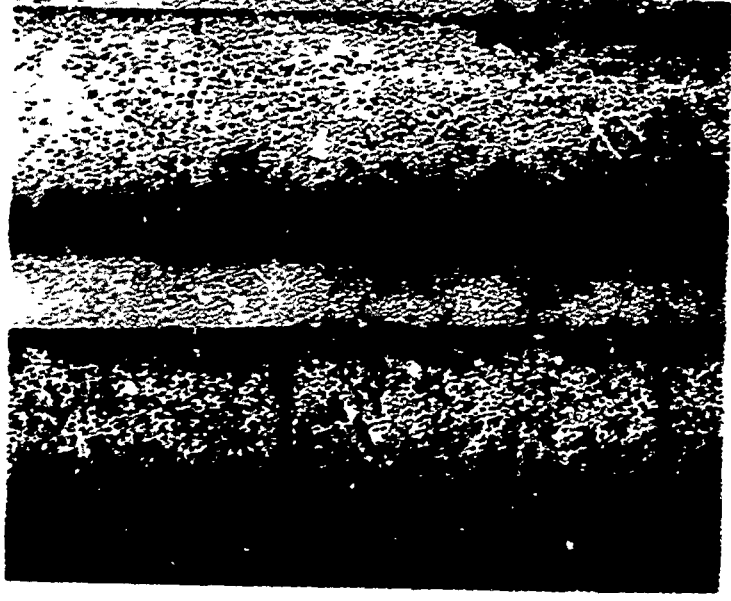
Wetting agent (Plastiment) 1 percent of cement weight.

To withstand the tensile stresses to be applied in the tests, the mortar rods were provided with a 3/16-inch steel rod passing through the center, each end of which was threaded into a 1/2-inch diameter coupling section. The mix was placed in a plexiglass mold, thoroughly rodded, and then cured for 8 hours. The mortar rods fabricated in this manner had very smooth surfaces. Some of the rods were roughened by successive immersion in weak hydrochloric acid, washing, and scrubbing with a stiff brush until about 15 percent of the diameter of the sand grains was exposed above the level of the cement paste. Surface application of graphite or teflon was identical to that used on the steel rod.

The three rods, with no surface treatment, are shown in Figure 6.



(a) General View



100 1/4

(b) Close-up of Rough (Left) and Smooth (Right) Mortar Rods

FIG. 6. TEST RODS

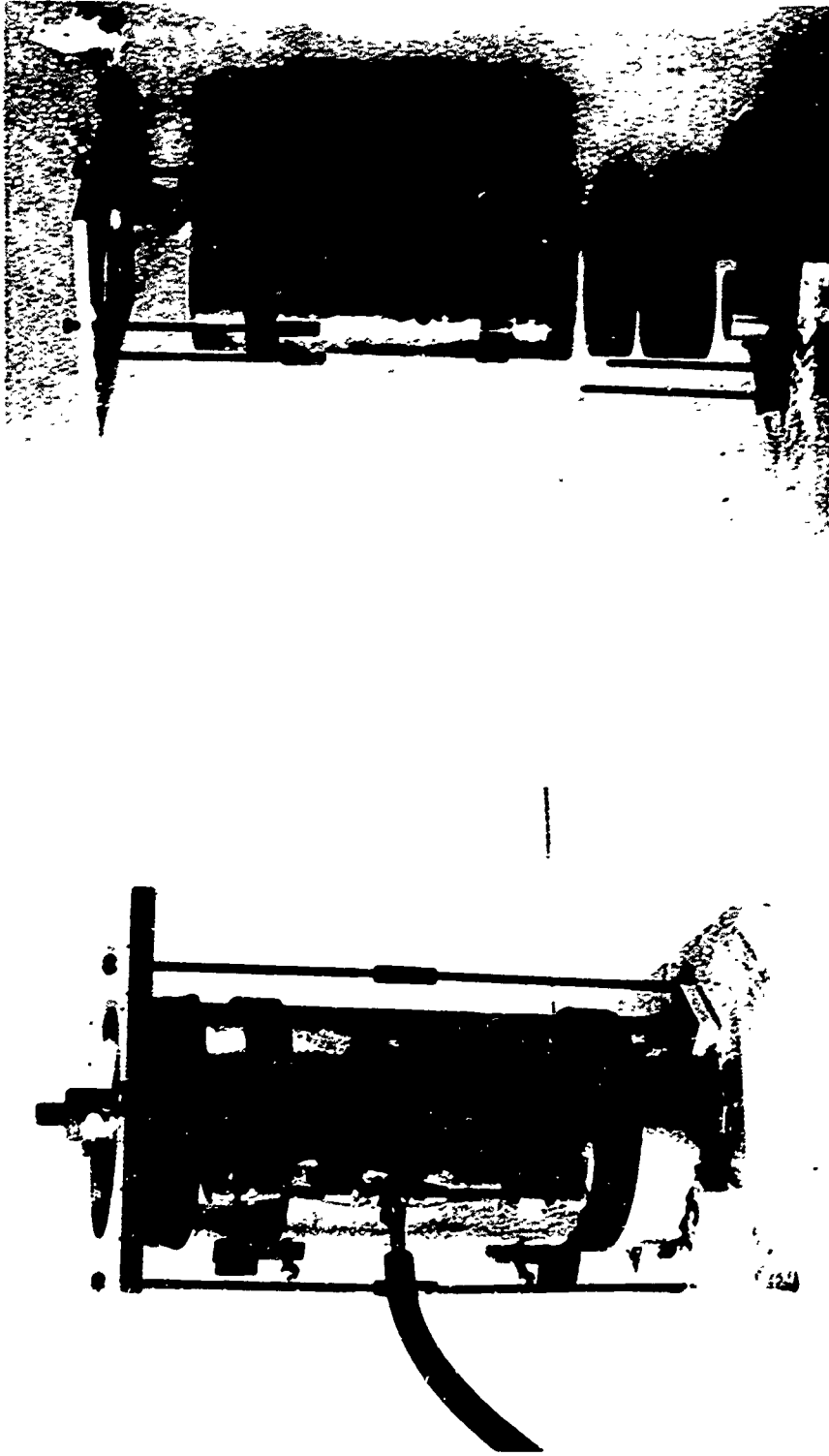
SECTION IV

APPARATUS AND PROCEDURES

1. SAMPLE PREPARATION

The rubber membrane used was 5 inches in diameter and 13 inches long with a thickness of about 0.015 inch. These membranes were fabricated using a single dip method (1). The filling mold consisted of a split brass casing 5 1/16 inches in diameter and 13 1/3 inches long (Figure 7), which was provided with a rubber gasket and two air evacuation ports. Two aluminum plates, 8 inches square, served as the top and bottom for the casing. To prepare the sample the test rod was pushed through the orifice in the rubber membrane and the assembly positioned inside the brass casing. Spacers were provided in the bottom of the mold so that the correct length of the sample would be obtained. A brass ring was placed around the top of the membrane; then the rubber was rolled back over the ring and some of the casing. The top plate was then screwed down over the rolled back membrane. With the split mold clamped shut a vacuum was applied to the volume between the membrane and the casing, which caused the membrane to be drawn tightly against the sides of the mold.

Both types of sand were placed by "raining" through a 5/8-inch diameter brass tube 18 inches long having a scattering screen at the bottom and a funnel at the top (Figure 8). The height of fall was regulated so that the diffusing screen always remained 4 to 6 inches above the surface of the sand. The rates of placement were 0.3 pound per minute for the 60-80 sand and 0.5 pound per minute for the 20-30 sand.



(a) Intact View

(b) Exploded View

FIG. 7. MOLD FOR SAMPLE PREPARATION



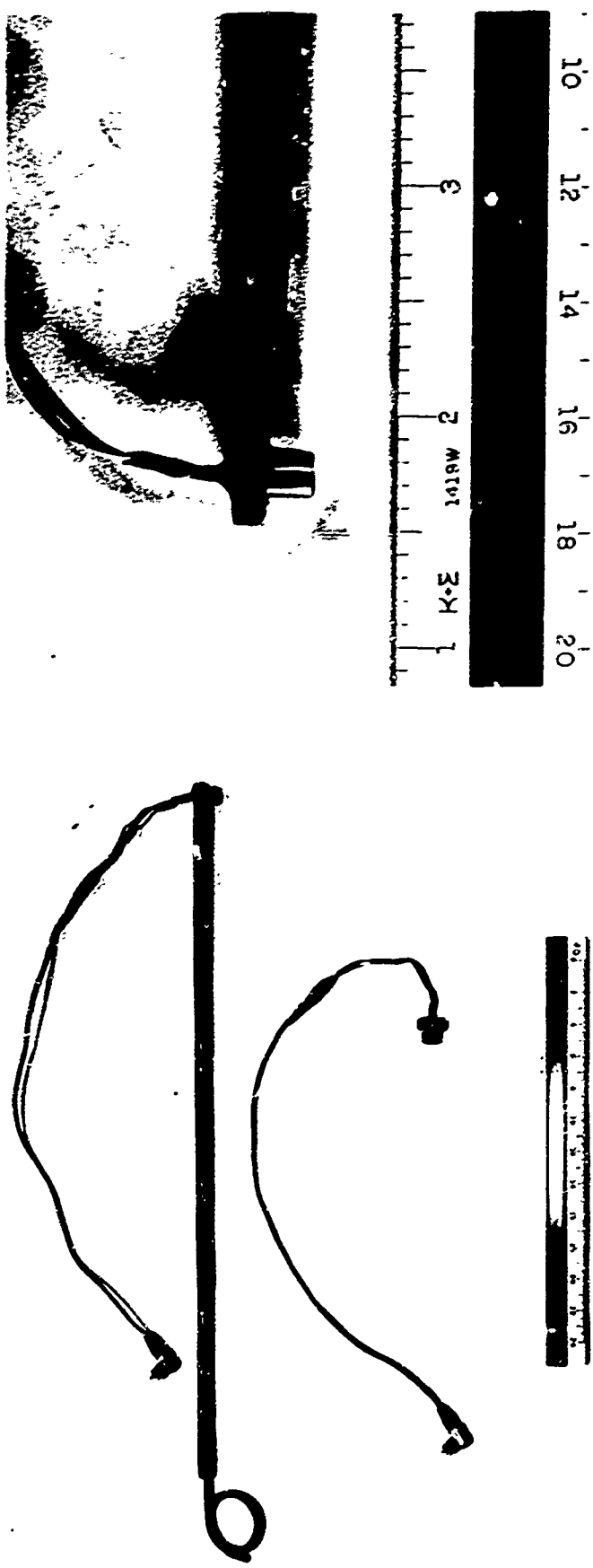
FIG. 8. SAND "RAINING" TUBE

When dynamic tests were being performed, the compaction process was stopped at various levels to allow for gage placement. The gage was secured in the positioning tool (Figure 9A), partially embedded in the sand with its face $1/4$ inch away from and normal to the rod and then released by means of the wire plunger. Gages were placed on opposite faces of the rod at stations 1 inch apart along the axis of the rod (Figure 9B). After each pair of gages were positioned, the raining process was resumed.

When the sand completely filled the mold, the vacuum applied to the side of the split mold was released. A headcap (Figure 10) was then placed over the upstream end of the rod. This headcap was fitted with twelve Microdot #33-53 bulkhead feed-thru adapters. In the dynamic tests the gage leads are screwed into the underside of the adapter, which provided a vacuum tight method of making an electrical connection through the rubber encased sample. With the gage leads connected, the headcap was pushed down until it seated on the surface of the sand. Also shown in Figure 10 are the evacuation ports through which the confining pressure was then applied to the sample.

The brass casing containing the sample was laid horizontally on a cradle, the screws maintaining the split mold were loosened, and the sample was carefully pushed from the casing (Figure 11). Also evident in these figures is the portable vacuum source employed. The extruded sample is shown in Figure 12.

Upon extrusion from the mold the sample was taken to the test area and placed in the sample housing (Figure 13), which consisted of a section of 8-inch-diameter cast iron pipe, $12\ 1/2$ inches long. The



(a) General View

(b) Close-up

FIG. 9A. STRESS GAGE AND GAGE PLACING TOOL



FIG. 9B. GAGE LOCATIONS

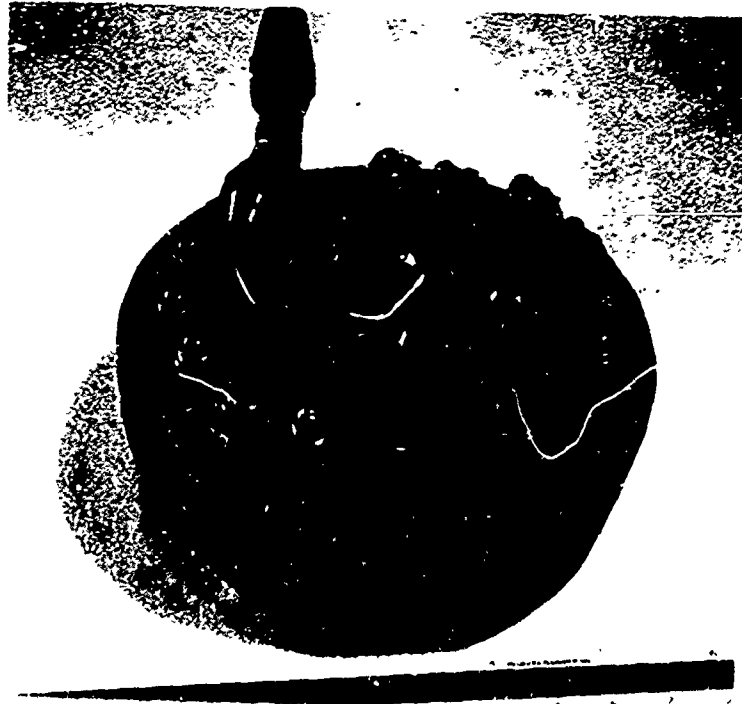
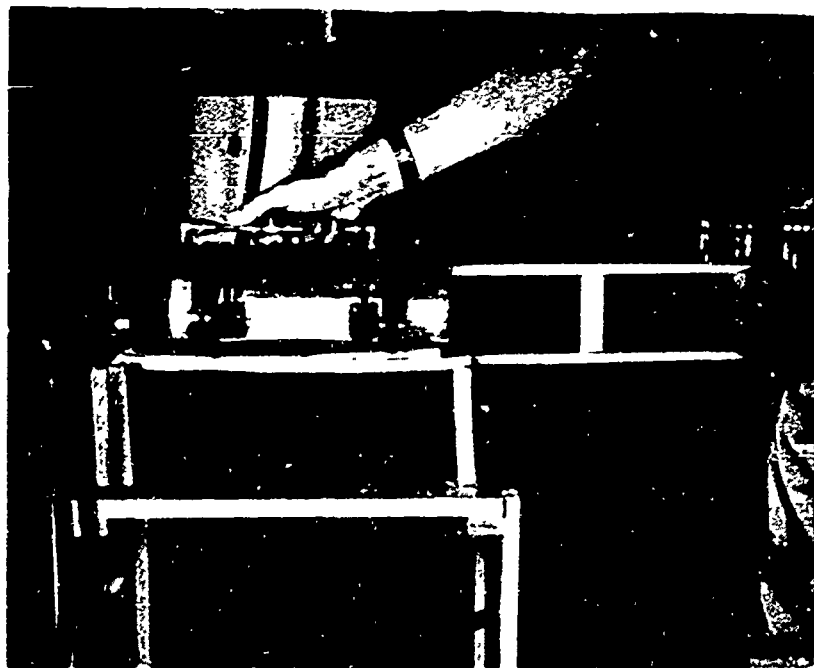


FIG. 10. SAMPLE HEADCAP



(a) Sample Ready for Extrusion (note portable vacuum source)



(b) The Extrusion Process

FIG. 11. EXTRUDING THE SAMPLE FROM THE MOLD

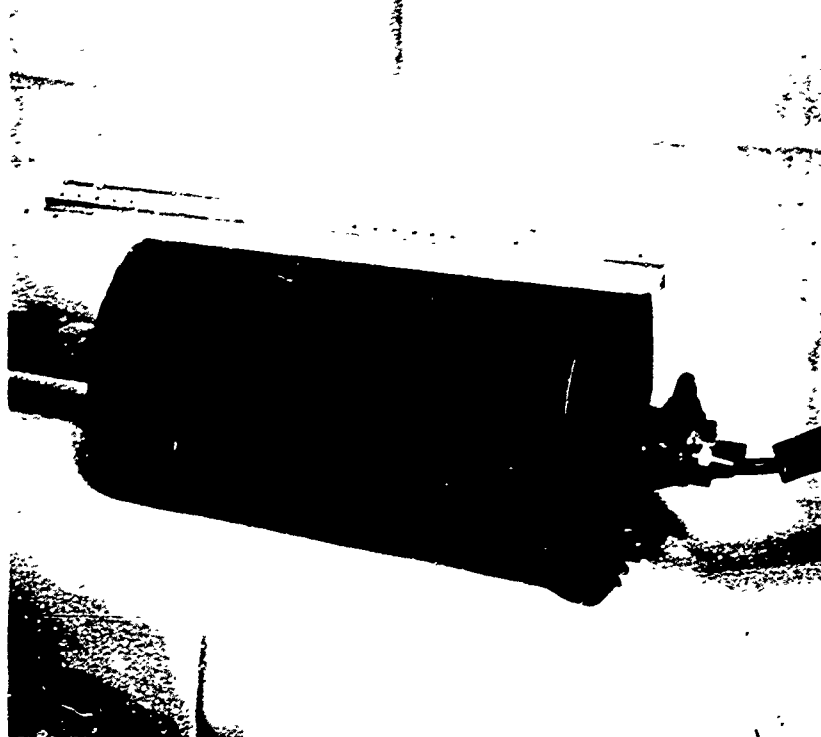


FIG. 12. THE EXTRUDED SAMPLE

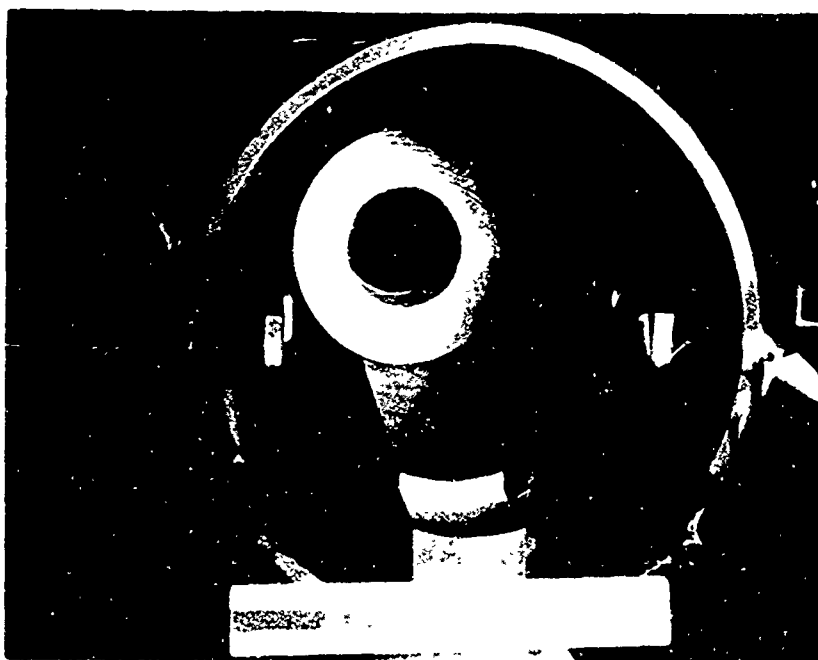


FIG. 13. SAMPLE HOUSING SHOWING ALIGNMENT GUIDES AND REACTION RING

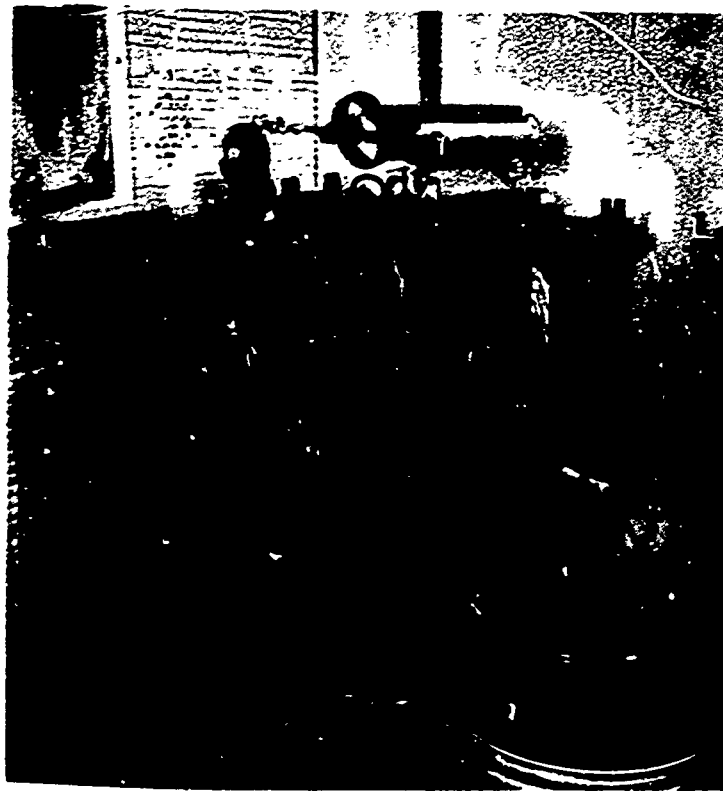
sample was supported on adjustable centering guides. At the downstream end of the housing was a 2-inch-thick wooden reaction ring, 5 inches O.D. and 2.5 inches I.D. The sample was slid into the housing until its downstream end came into contact with the reaction ring.

The sample housing was then placed on the test track and aligned with the shock tube and the cable used for the static tests by adjusting the contoured track. Once the housing was in position it was securely bolted to the test track. The sample was then ready for either static or dynamic tests.

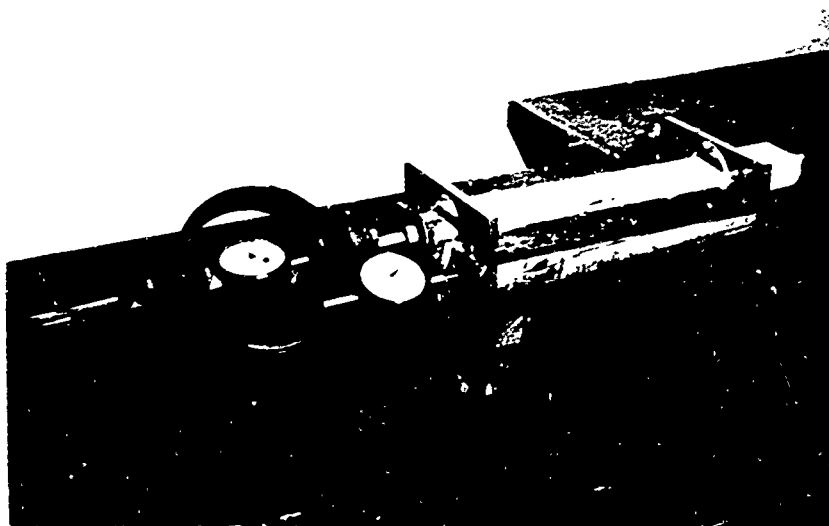
2. STATIC TESTS

To determine the relation between the confining pressure applied to the rod (when the membrane is evacuated) and the total normal force at the sand/rod interface, two auxiliary tests were conducted. The first of these consisted of a smooth steel plate upon which a single-grain layer of sand was cemented. A 6 inch x 6 inch mortar plate was placed on the sand and a normal force applied by means of weights (Figure 14a). The static friction force required to initiate slip was then measured by siphoning water into the loading bucket, whence the value of μ_s was obtained.

In the second auxiliary test a sawed 2-inch diameter mortar rod was embedded in the sand with its flat surface up (Figure 14b) and normal loads were applied to this upper surface (the sand was restrained from heaving by metal plates). A static friction test was performed and a second value of μ_s computed.



(a) Flat-Plate Test (connected to Static Pull System)



(b) Split-Rod Test (Normal Load N Removed)

FIG. 14. APPARATUS FOR AUXILIARY STATIC FRICTION TESTS

The test sample prepared as previously described was mounted on the test track, the rod was attached to the proving ring and loading cable, and the displacement dial was clamped in place (Figure 15). Load was applied by siphoning water into the loading bucket at a rate which would produce slip in about 5 minutes while load and displacement dial readings were taken. Once slip occurred, further displacement was prevented. After the "virgin" pull, the load bucket was emptied and "repull" tests were conducted at three different confining pressures.

3. DYNAMIC TESTS

After mounting and aligning the sample on the test track, the piston assembly on which the shock wave impinges to transfer the forcing function to the rod was then set in place (Figure 16); the piston rod and test rod were separated by a thin rubber gasket and kept in contact by means of springs.

The body of the LVDT used to measure the velocity of the test rod (Appendix B) was clamped to supports in front of the housing and its core threaded to the end of the test rod (Figure 17). The assembly is shown in Figure 18. A detail of the gage connections through the rubber headcap is shown in Figure 19. Single sweep, dual trace oscilloscopes were used to record the piezoelectric gage outputs. Details for gage fabrication, calibration, and recording circuitry may be found in Reference 3. Figure 20 is a general view of the dynamic test set up.

Two series of dynamic tests were run. One series had all the stress gages in a horizontal plane, six gages on the left side and six on the right side. The second series had all the stress gages in a vertical plane, six gages on top and six on the bottom. To facilitate

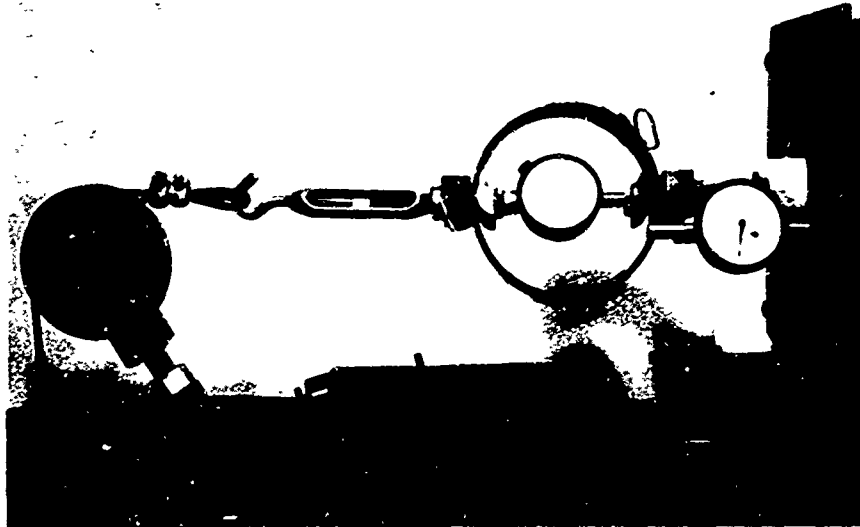


FIG. 15. PROVING RING AND DISPLACEMENT DIAL IN POSITION FOR STATIC TEST

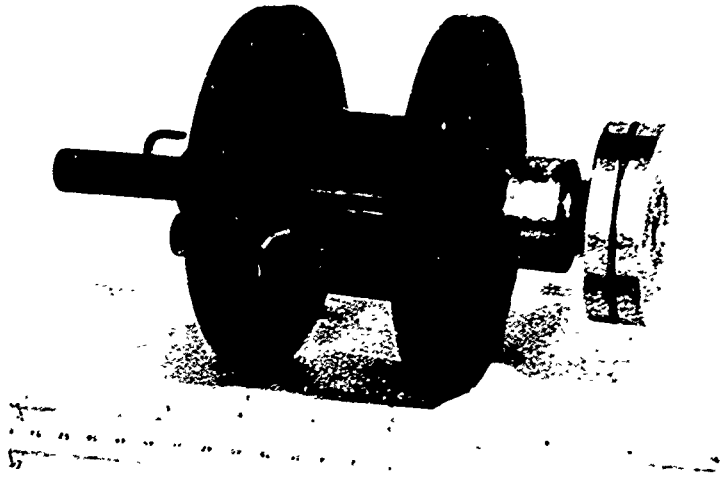


FIG. 16. PISTON ASSEMBLY

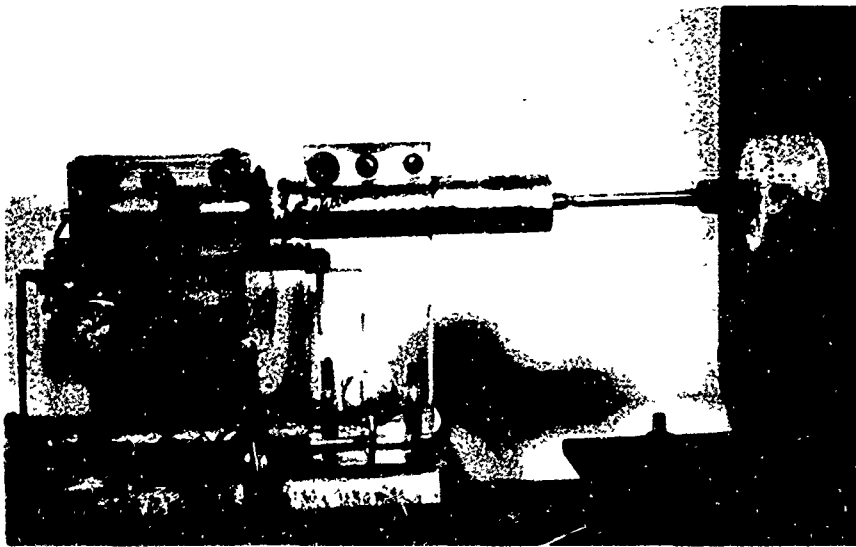


FIG. 17. LVDT MOUNTING



FIG. 18. DYNAMIC TEST ASSEMBLY

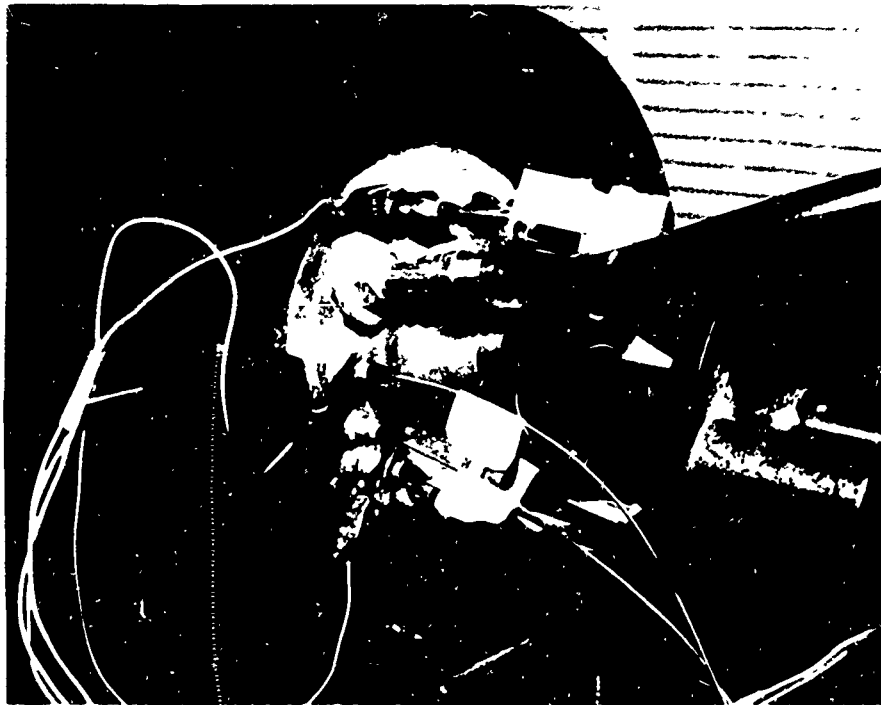


FIG. 19. DETAIL OF HEADCAP



FIG. 20. GENERAL VIEW OF DYNAMIC TEST SET-UP

comparison between successive tests, it was decided to position the gages at the same stations. The spacing selected was 3, 4, 5, 6, 7, and 8 inches from the headcap.

In both series of tests, the piezoelectric pressure gages were placed with their sensitive elements facing the rod but $1/4$ inch away from it (Figure 9B). Tests showed that the pressure did not attenuate appreciably with distance from the rod out to a distance of $1/2$ inch; when the spacing became $1/8$ inch or less the gage output became very erratic.

To evaluate the inertial response of the piezoelectric gages, plexiglass caps were placed over the sensitive faces of the gages prior to embedment (Figure 21). A series of tests was performed using the capped gages.

It was found that $1/16$ inch of rod movement was necessary to insure rod/sand slip; this usually took 3-4 milliseconds after rod movement started. However, if a static test was first performed, rod/sand slip occurred after 1.4-1.8 milliseconds, or with about 0.01 inch of rod movement. To compare static and dynamic coefficients of friction under the same test conditions, each of the dynamic tests was preceded by a static test.

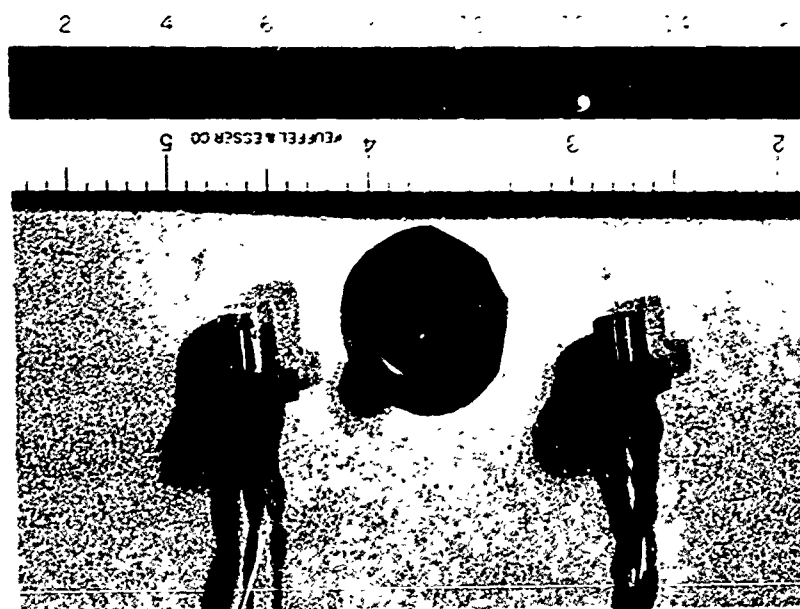


FIG. 21. CAPPED STRESS GAGE (left)

SECTION V

RESULTS

1. STATIC FRICTION TESTS

The values of the coefficient of static friction, μ_s , computed from the auxiliary tests and those computed from the solid rod tests -- assuming that the contact pressure at the sand/rod interface, σ_a , equals the confining pressure, σ_m , on the membrane -- are compared in Table III. It was concluded from these results that, for all practical purposes, it may be assumed that $\sigma_a = \sigma_m$ and this assumption was made in interpreting the remainder of the static friction tests. The only other study that could be found relevant to this question was made by Kennedy (4) who worked with a 16-inch-diameter membrane-encased sand sample having a concentric 7-inch-diameter steel pipe. Kennedy concluded that $\sigma_a = 1.4 \sigma_m$ for his conditions.

Typical relationships between the applied frictional force and rod displacement obtained from the static tests are shown in Figures 22 through 24. Although the displacement required to induce slip in the virgin pull always exceeded that in the repull tests -- sometimes by significant amounts -- the ultimate value of the friction force is the same for the two cases. Accordingly, it was felt that preceding the dynamic test by a static test should not alter the value of μ_t that would be obtained and would provide test data under essentially the same initial conditions.

Tables IV and V summarize the values of μ_s obtained for the two sands on the variety of surfaces tested (sample calculations may be

TABLE III
 COMPARISON OF μ_s VALUES FOR DIFFERENT TYPES OF TESTS WITH 20-30 SAND

Type of Surface	Flat-Plate Test	Split-Rod Test	Solid Rod Test Assuming $\sigma_m = \sigma_a$	
			2 Inch Rod	1 1/8 Inch Rod
Smooth Mortar	0.54	0.59	0.52	0.65
Teflon	0.38	0.43	0.34	0.31
Graphite	0.35	0.42	0.34	0.30

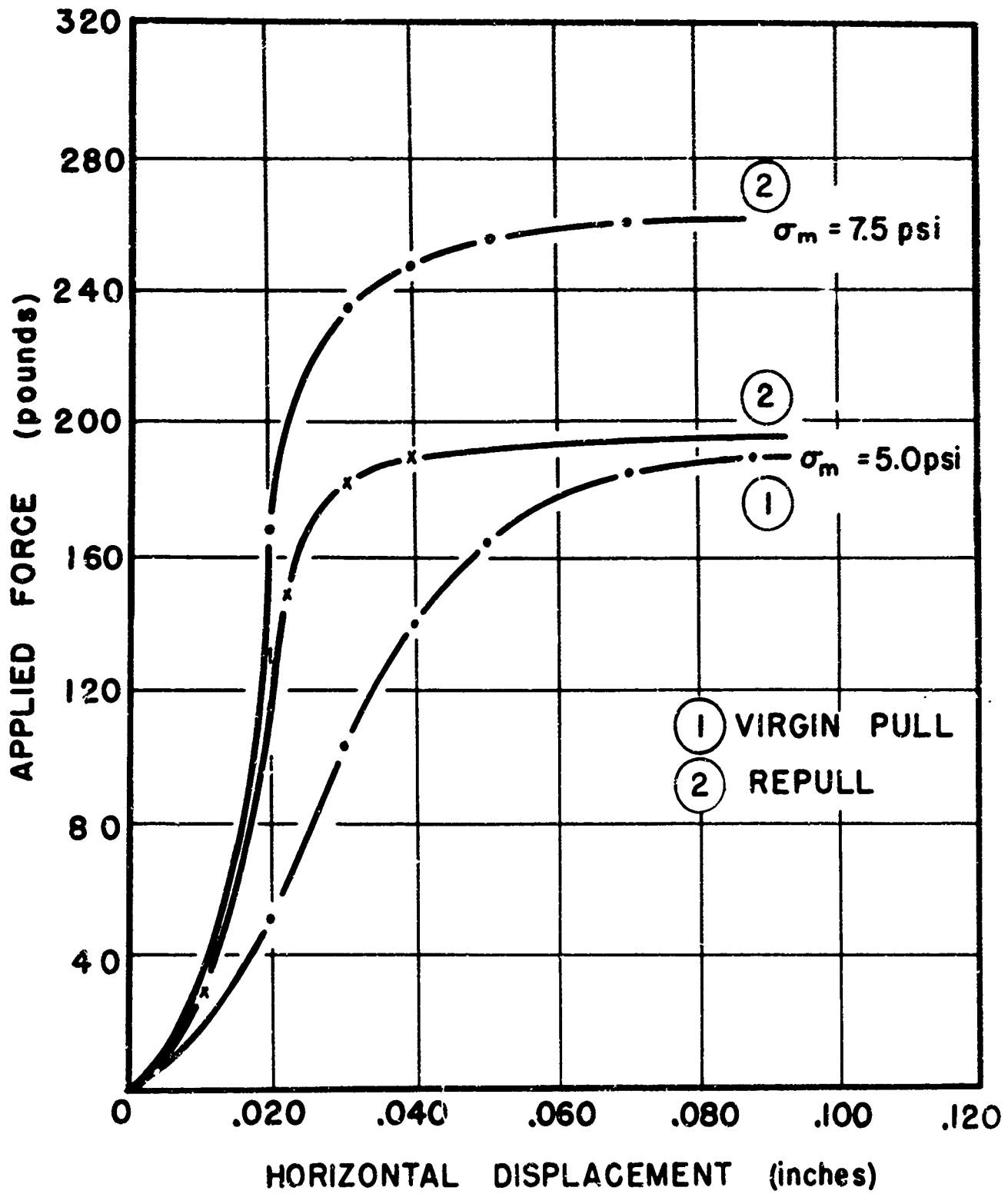


FIG. 22 FORCE vs DISPLACEMENT FOR 60-80 SAND ON PLAIN SMOOTH MORTAR (static test No. 7)

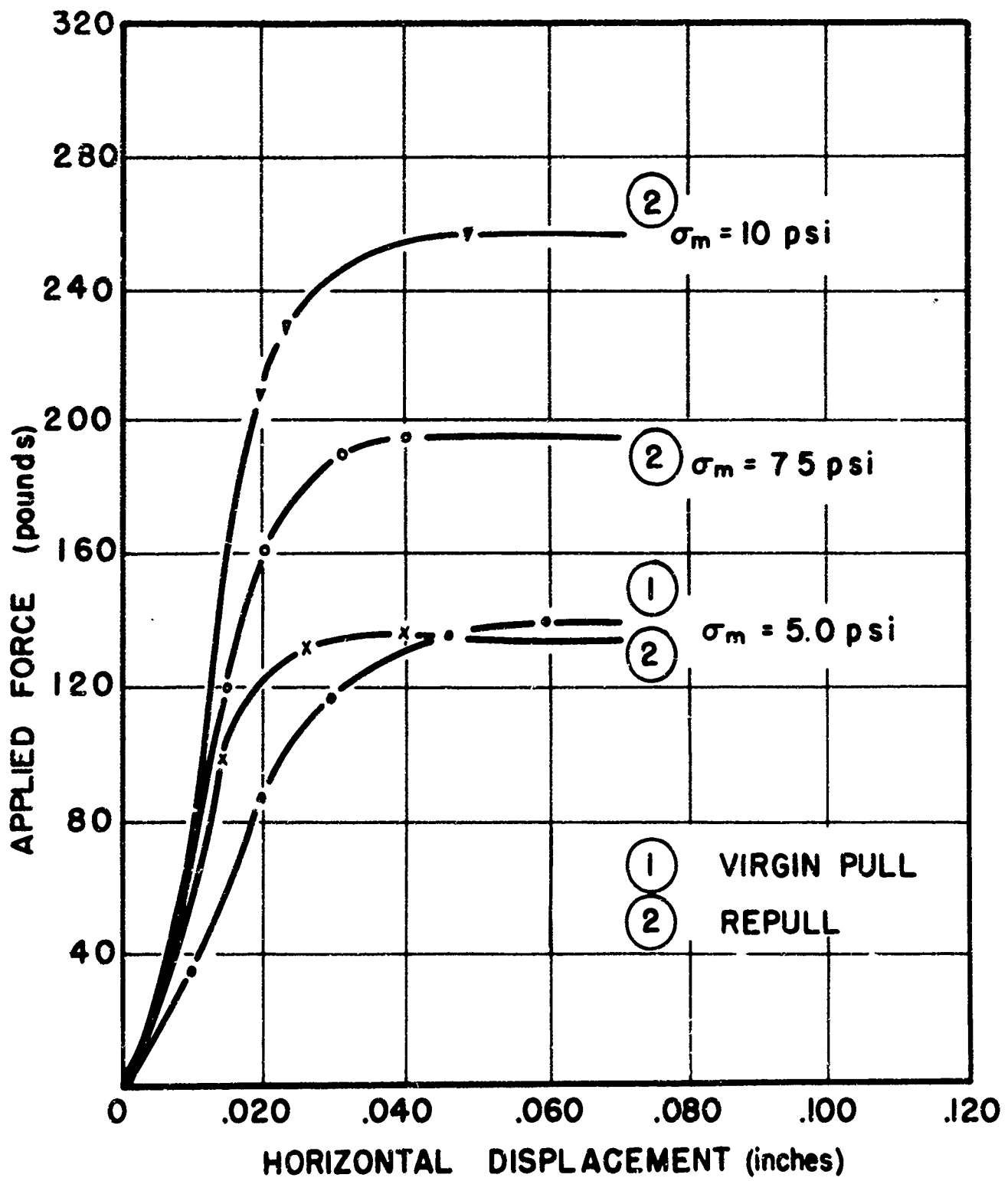


FIG. 23 FORCE vs DISPLACEMENT FOR
20-30 SAND ON PLAIN ROUGH MORTAR
(static test No. 14)

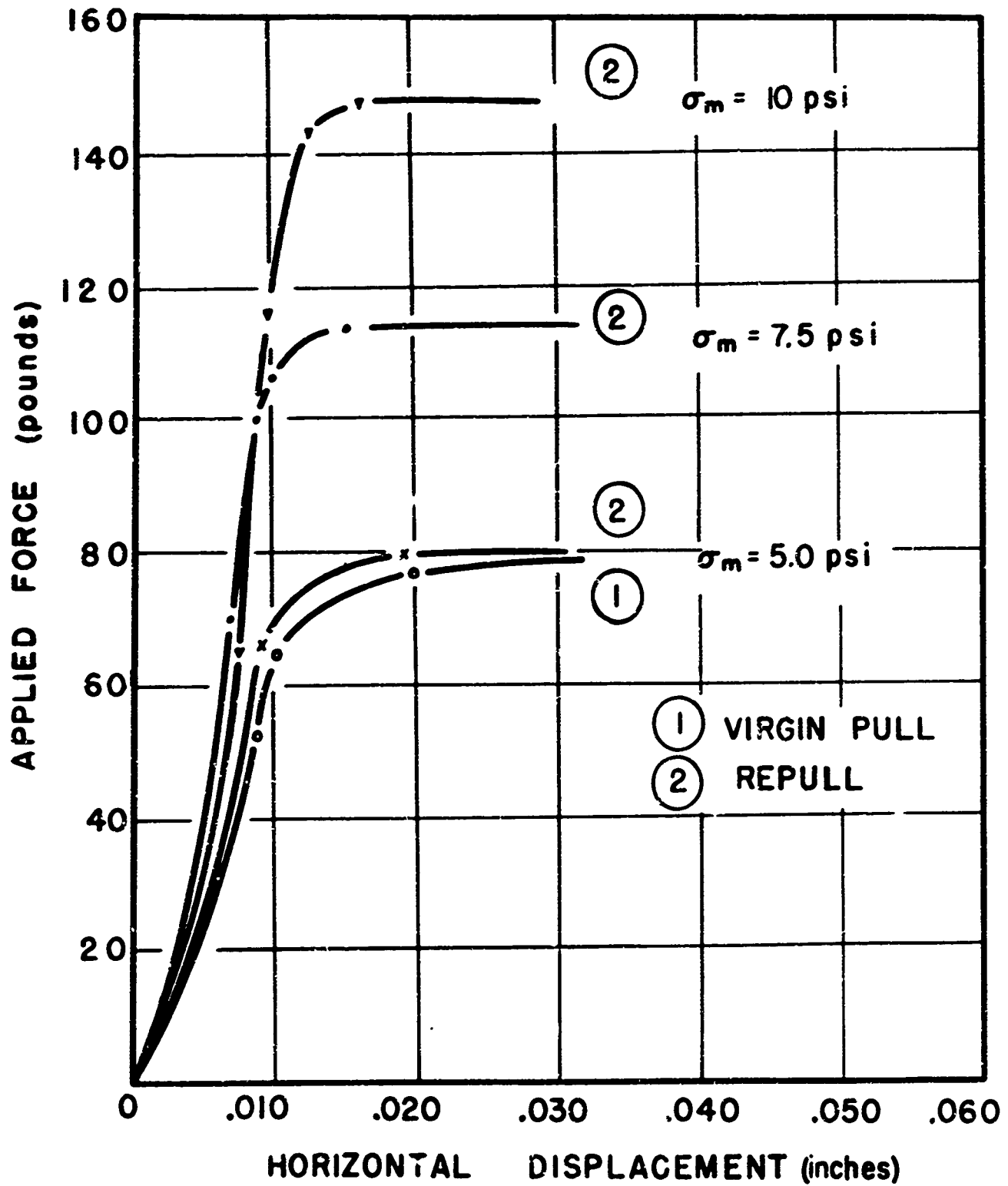


FIG. 24 FORCE vs DISPLACEMENT FOR 20-30 SAND ON TEFLON COATED STEEL (static test No. 15)

TABLE IV

VALUES OF μ_s BASED ON STATIC TESTS WITH 60-80 SAND

Static Test No.	Rod Surface	$\sigma_m = 5 \text{ psi}$			$\sigma_m = 7.5 \text{ psi}$			$\sigma_m = 10 \text{ psi}$		
		Virgin	Repull	Repull	Repull	Repull	Repull	Repull	Repull	Repull
2	Plain Steel	0.52	0.50	0.49	0.49	0.49	0.49	0.49	0.49	0.50
8	Plain Steel	0.51	0.49	0.49	0.49	0.49	0.49	0.49	0.49	0.50
7	Plain Smooth Mortar	1.06	1.09	1.09	1.09	1.09	1.09	1.09	1.09	1.09
1	Plain Rough Mortar	1.12	-----	-----	-----	-----	-----	-----	-----	-----
3	Plain Rough Mortar	1.26	1.25	1.25	1.25	1.25	1.25	1.25	1.25	1.25
5	Teflon Coated Steel	0.66	0.57	0.57	0.57	0.57	0.57	0.57	0.57	0.57
12	Teflon Coated Steel	0.66	0.64	0.64	0.64	0.64	0.64	0.64	0.64	0.64
13	Teflon Coated Steel	0.66	0.58	0.58	0.58	0.58	0.58	0.58	0.58	0.58
9	Graphite Coated Steel	0.39	0.37	0.37	0.37	0.37	0.37	0.37	0.37	0.37
19	Teflon Coated Smooth Mortar	0.69	0.57	0.57	0.57	0.57	0.57	0.57	0.57	0.57
11	Graphite Coated Smooth Mortar	0.73	0.61	0.61	0.61	0.61	0.61	0.61	0.61	0.61

$\tan \phi' = 1.11$

TABLE V
VALUES OF μ_s BASED ON STATIC TESTS WITH 20-30 SAND

Static Test No.	Rod Surface	$\sigma_m = 5$ psi		$\sigma_m = 7.5$ psi		$\sigma_m = 10$ psi	
		Virgin	Repull	Repull	Repull	Repull	Repull
16	Plain Steel	0.35	0.34	0.35	0.35	0.35	0.35
20	Plain Steel	0.33	0.32	0.35	0.35	0.36	0.36
18	Plain Smooth Mortar	0.62	0.62	0.59	0.59	0.59	0.59
14	Plain Rough Mortar	0.79	0.76	0.72	0.72	0.70	0.70
15	Teflon Coated Steel	0.33	0.33	0.32	0.32	0.32	0.32
24	Teflon Coated Smooth Mortar	-----	0.33	0.35	0.35	0.33	0.33
17	Graphite Coated Steel	0.22	0.23	0.24	0.24	0.26	0.26
25	Graphite Coated Smooth Mortar	-----	-----	0.31	0.31	0.32	0.32

$\tan \phi' = 0.84$

found in Appendix C). It will be noted that tests were repeated to check reproducibility. The agreement found was excellent in all cases, even when different investigators performed the tests. Examination of the data shows that the coefficient of wall friction depends not only on the nature of the surface involved but also on the angularity and roughness of the sand grains in relation to the roughness of the surface itself. In the case of the 60-80 sand sliding on the rough mortar rod the angle of wall friction essentially equalled the angle of shearing resistance of the sand, which implies sand/sand slip. Under "static" conditions, graphite was found to be an effective lubricant for all types of surfaces tested; this was also true for Teflon, with the exception of the polished steel surface.

Suklje and Brodnik (5) performed static friction tests with several flat concrete plates 20 cm. in width and either 60 cm. or 30 cm. long on beds of two types of cohesionless material. Their test results show that the coefficient of static friction between a smooth concrete plate and gravel is less than between the same plate and sand, and that μ_s for a rough concrete plate sliding on gravel is greater than a smooth concrete plate sliding on the same gravel. Since details of the nature of the cohesionless materials or the roughness of the concrete plates were not given, direct comparison of numerical values with those obtained in this study is not possible. However, the order of magnitude of the results obtained, and their general trends are comparable.

Potyondy (6) performed skin friction tests with steel, concrete, and wood on various soils. The tests were run in a stress controlled

shear box which had an area of 12.4 sq. in. The steel test surface was very similar to the one used in this study; the smooth concrete surface was prepared by placing a concrete mix with 2.5 mm maximum aggregate in a plywood form; and the rough concrete surface was made by pouring a mix with 7.5 mm maximum aggregate on "flat rough ground." Among the soils tested by Potyondy was a well graded sand having a uniformity coefficient of 3.8 and a median size corresponding to the 20-30 sand. The results obtained are compared in Table VI.

TABLE VI
COMPARISON OF μ_s VALUES

<u>Item</u>	<u>Potyondy</u>	<u>20-30 Sand</u>
Relative Density (%)	66	92
Normal stress	7.0	7.5
$\tan \phi$	0.98	0.84
μ_s smooth steel	0.45	0.35
smooth concrete	0.82	0.59
rough concrete	0.97	0.72

2. DYNAMIC TESTS

Figure 25 shows a typical output trace obtained from the LVDT. At the lower left hand corner of the photograph a sharp downward "blip" is observed; this is the output from the time mark generator. About 1.1 ms later, the shock wave impinged on the piston assembly and transferred the forcing function to the test rod and surrounding sand, thereby accelerating the entire assembly. Then, as the force built up against the reaction ring, the rod velocity became constant until rod/sand slip occurred (about 1.7 ms after the forcing function first

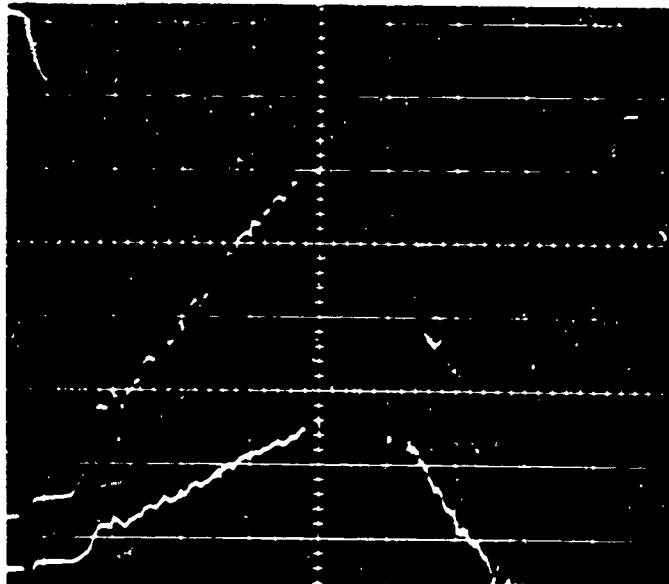


FIG. 25. TYPICAL LVDT TRACE (Shot 2000R)

Sweep 2 ms/cm sensitivity: Top = 0.02 volts/cm
Bottom = 0.05 volts/cm

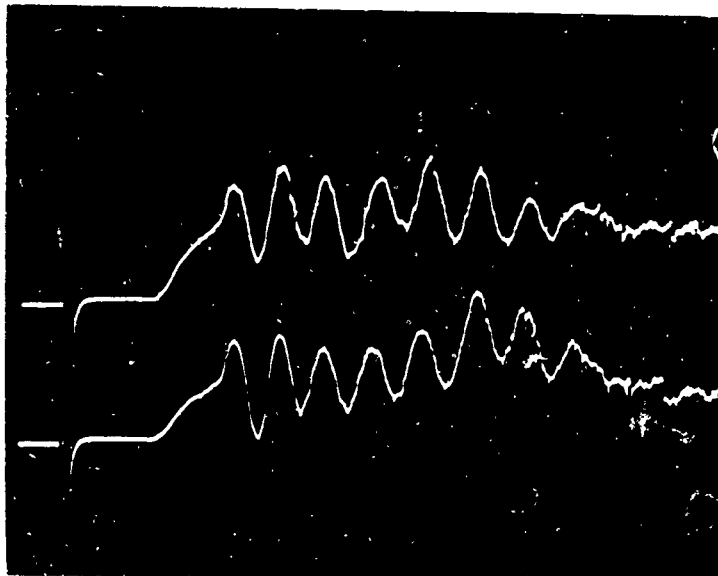


FIG. 26. TYPICAL PRESSURE GAGE TRACE (Shot 1306, uncapped)

Top: Gage #1 scale; 1 ms/cm, 0.05 volts/cm
Bottom: Gage #2

caused the rod to accelerate). At this time, the magnitude of the forcing function was 185 pounds (Figure 2, 40 psig). Thereafter, the acceleration was essentially constant, and since the forcing function increased slightly with time (until it decayed sharply at 7 ms) it may be inferred that the coefficient of dynamic friction increased slightly with velocity (about 10%, for velocities up to about 30 inches/sec). The slope of the velocity-time trace after slip occurred was used to obtain the acceleration of the rod in order to compute the inertia force.

Figure 26 shows typical traces from a pair of uncapped pressure gages. The time mark and the instant at which the forcing function impinges on the rod are clearly evident. About 0.8 ms after this time (i.e. when the reaction ring had picked up its load, but before rod/sand slip took place) a 1200-1500 cycle/sec disturbance developed in the gage outputs and continued until the forcing function decayed. This phenomenon was also observed in the capped gages, although the amplitude of the disturbance was less pronounced. The cause of the disturbance is not understood, but to interpret the record a smooth curve was drawn through the mean amplitude of the trace. A time of 2 ms was selected for computation purposes; a) because this time is just slightly beyond that at which rod/sand slip occurred in all the tests, b) the forcing function was constant between slip and 2 ms, and c) the acceleration of the rod could be determined reliably at this time. Having obtained the gage factors by calibration (3) the gage response could be expressed as a pressure for each station along the rod. A typical result, averaging top and bottom gages, is shown in Figure 27.

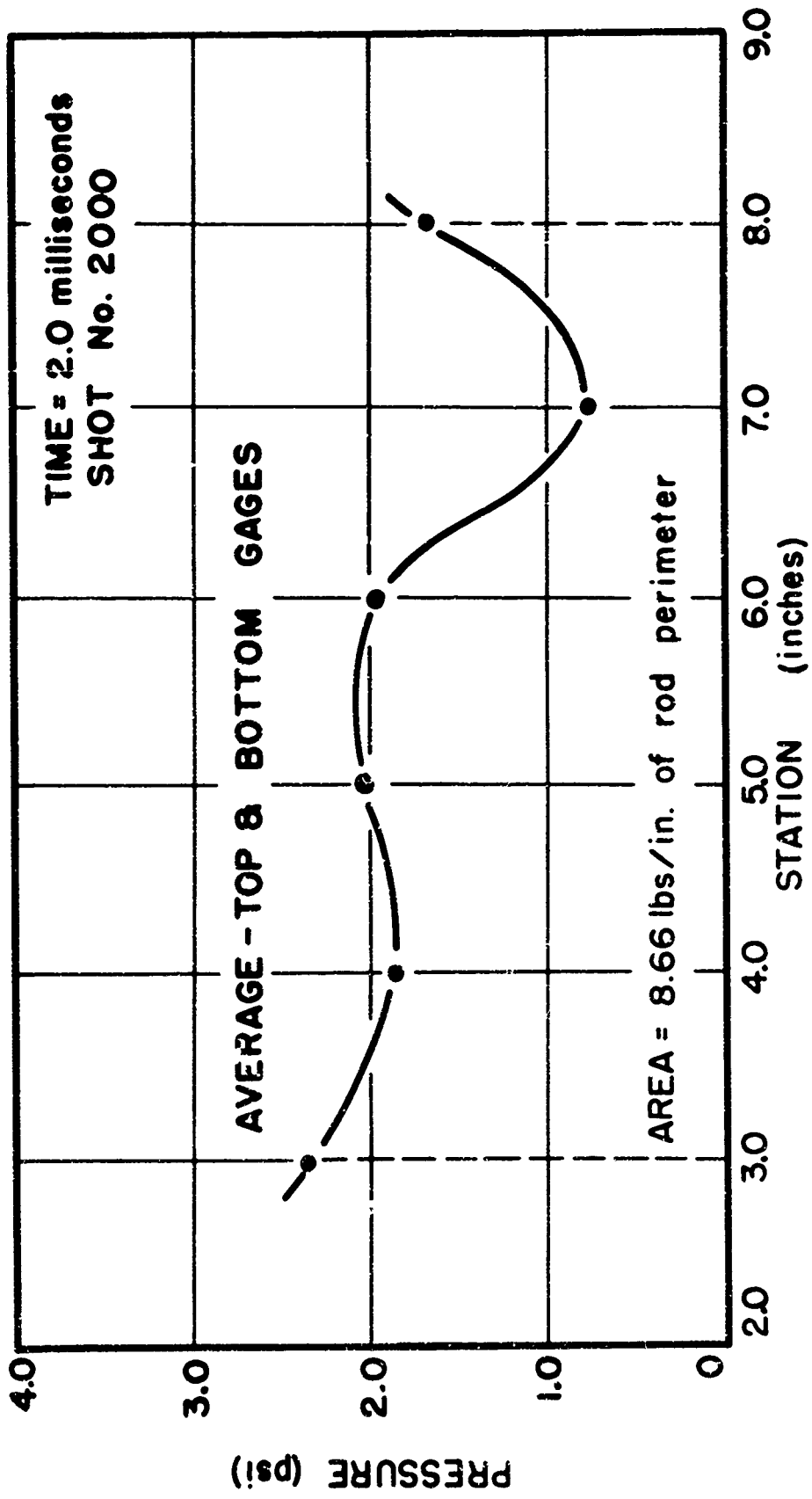


FIG. 27 ΔN vs STATION ALONG ROD (at slip)

Assuming that the middle 5 inches is typical of the pressure changes that might be taking place along the 10-inch length of rod, the apparent change in normal force (ΔN_s) could be computed. Table VII gives the values of ΔN_s calculated in this manner for the tests with capped and uncapped gages, respectively. Although indications are that a small increase in normal force does develop before slip occurs, it is not large enough to influence the computed values of μ_d significantly. Accordingly, the values of μ_d reported in Tables VIII to XIII were computed assuming ΔN_s equals zero. The data are indicative of the reproducibility in test results that was achieved. Table XIV summarizes the average values of μ_d that were obtained and compares them with the corresponding values of μ_s . The results show that the coefficient of dynamic friction is greater than the static friction. In the case of unlubricated surfaces, the increase is of the order of 25 percent unless sand/sand slip occurs. The data in Table XIV offer further evidence that ϕ' dynamic essentially equals ϕ' static; thus, $\tan \phi'$ is an upper limiting value for the coefficient of friction that can be developed in drained sands.

Tables IV and V show that graphite is an excellent lubricant under static conditions; Teflon is effective when compared with the plain mortar surfaces but increased friction slightly in the case of the smooth steel surface. They still act as lubricants under dynamic conditions especially in the case of graphite; but Teflon is much less efficient, due perhaps to viscosity effects.

TABLE VII

 ΔN_s FOR UNCAPPED AND CAPPED GAGES AT TIME OF SLIP

Material: Plain Steel
 $F(t) = 185$ lbs.
 Confining Pressure = 5 psi

<u>From</u> <u>Gages Positioned on</u> <u>Left and Right of Rod</u>			<u>From</u> <u>Gages Positioned on</u> <u>Top and Bottom of Rod</u>		
Test No.		ΔN_s (Lb.)	Test No.		ΔN_s (Lbs)
1306	Uncapped	47	2000	Uncapped	80
1309	Uncapped	52	2001	Uncapped	63
1310	Uncapped	42	2002	Uncapped	96
1311	Uncapped	44	2003	Uncapped	74
1312	Uncapped	51			
		<hr/>			<hr/>
Average		47	Average		78
1313	Capped	36	2004	Capped	91
1314	Capped	28	2005	Capped	77
		<hr/>			<hr/>
Average		32	Average		84

TABLE VIII

VALUES OF μ_d FOR 60-80 SAND ON PLAIN STEELForcing Function: $F(t) = 185$ lbs.Confining Pressure: $\sigma_m = 5$ psiMass: $m = 1.43 \times 10^{-2}$ lbs. sec²/in.

Test No.	$N_d = N_s$ (Lbs)	ma (Lbs)	F_d (Lbs)	μ_d
2000	214	37	148	0.69
2001	214	41	144	0.67
2002	214	59	126	0.59
2003	214	--	---	---
2004 Capped	214	43	142	0.66
2005 Capped	214	33	152	0.71
2000 R*	214	44	141	0.66
2001 R	214	55	130	0.61
2002 R	214	52	133	0.62
2003 R	214	48	137	0.64
2004 F Capped	214	38	147	0.69
2005 H Capped	214	46	139	0.65
1306	214	46	139	0.65
1309	214	28	157	0.73
1310	214	63	122	0.57
1311	214	51	134	0.63
1312	214	--	---	---
1313 Capped	214	56	129	0.60
1314 Capped	214	39	146	0.68
1309 R*	214	55	130	0.61
1310 R	214	98	87	0.41
1311 R	214	--	---	---
1312 R	214	55	130	0.61
1313 R Capped	214	50	135	0.66
1314 R Capped	214	43	142	0.66
Average				0.63

* R designates a reshot

TABLE IX

VALUES OF μ_d FOR 20-30 SAND ON SMOOTH MORTAR

1 1/8" Dia. Rod; Weight of Moving System = 2.71 lbs.

Test No.	N_s (Lbs)	ma (Lbs)	$F(t)$ (Lbs)	F_d (Lbs)	μ_d
73DS	168	65	185	120	0.71
48DS	168	54	185	131	0.78
49DS	168	35	185	150	0.89
52DS	168	68	185	117	0.70
53DS	168	71	185	114	0.68
56DS	210	86	220	134	0.64
57DS	210	40	185	145	0.69
74DS	210	76	220	144	0.68
38DS	252	67	220	153	0.61
39DS	252	75	220	145	0.58
60DS	336	49	275	226	0.67
61DS	336	87	275	188	0.55
62DS	336	55	275	220	0.66
63DS	336	72	275	203	0.60
76DS	336	43	275	232	0.69

2" Dia. Rod; Weight of Moving System = 5.29 lbs.

127DS	300	63	220	157	0.52
129DS	300	52	275	223	0.74
136DS	300	67	275	208	0.69
Average					0.67

TABLE X

VALUES OF μ_d FOR 20-30 SAND ON ROUGH MORTAR

1 1/8" Dia. Rod; Weight of Moving System = 2.70 lbs.

Test No.	N_s (Lbs)	ma (Lbs)	F(t) (Lbs)	F_d (Lbs)	μ_d
40DS	168	57	220	163	0.97
41DS	168	58	220	162	0.97
77DS	168	56	220	164	0.98
83DS	210	40	220	180	0.86
64DS	210	66	220	154	0.73
65DS	210	67	220	153	0.73
79DS	252	43	275	232	0.92
82DS	294	22	275	253	0.86
111DS	294	45	275	230	0.78
112DS	294	45	275	230	0.78
70DS	294	78	275	197	0.67
71DS	294	58	275	217	0.74

2" Dia. Rod; Weight of Moving System = 5.29 lbs.

185DS	300	53	275	222	0.74
186DS	300	53	275	222	0.74

Average

0.82

TABLE XI

VALUES OF μ_d FOR 20-30 SAND ON TEFLON COATED SMOOTH MORTAR

2" Dia. Rod; Weight of Moving System = 5.29 lbs.

Test No.	N_s (Lbs)	ma (Lbs)	F(t) (Lbs)	F_d (Lbs)	μ_d
159DS	300	94	275	181	0.60
160DS	300	113	275	162	0.54
161DS	300	40	220	180	0.60
Average					0.58

TABLE XII

VALUES OF μ_d FOR 20-30 SAND ON TEFLON COATED STEEL

1 1/8" Dia. Round Rod; Weight of Moving System = 5.52 lbs.

Test No.	N_s (Lbs)	ma (Lbs)	F(t) (Lbs)	F_d (Lbs)	μ_d
90DS	168	65	185	120	0.71
91DS	168	67	185	118	0.70
92DS	168	69	185	116	0.69
105DS	210	106	220	114	0.54
106DS	210	115	220	105	0.50
113DS	210	103	220	117	0.56
93DS	252	86	220	134	0.53
94DS	252	73	220	147	0.58
95DS	252	83	220	137	0.54
107DS	294	78	220	142	0.48
108DS	294	81	220	139	0.47
109DS	294	79	220	141	0.48
96DS	336	92	275	183	0.55
97DS	336	85	275	190	0.57
110DS	336	106	275	169	0.50
Average					0.56

TABLE XIII

VALUES OF μ_d FOR 20-30 SAND ON GRAPHITE COATED SMOOTH MORTAR

1 1/8" Dia. Rod; Weight of Moving System = 2.71

Test No.	N_s (Lbs)	ma (Lbs)	$F(t)$ (Lbs)	F'_d (Lbs)	μ_d
151DS	210	81	185	104	0.49
165DS	210	76	185	109	0.52
152DS	210	84	185	101	0.48
144DS	252	46	185	139	0.55
145DS	252	77	185	108	0.43
149DS	252	61	185	124	0.49
147DS	336	77	220	143	0.43
146DS	336	99	275	176	0.52
148DS	336	48	185	137	0.41
140DS	420	88	275	187	0.45
142DS	420	75	275	197	0.47
141DS	420	37	220	183	0.44

2" Dia. Rod; Weight of Moving System = 5.29 lbs.

174DS	300	94	220	121	0.42
175DS	300	94	220	126	0.42
176DS	300	82	220	138	0.46
179DS	450	118	275	157	0.35
178DS	450	109	275	166	0.37
177DS	450	112	275	163	0.36
183DS	525	88	275	187	0.36
189DS	525	92	275	183	0.35

Average 0.44

TABLE XIV
 COMPARISON OF STATIC AND DYNAMIC COEFFICIENTS OF FRICTION

Rod Surface	Sand	μ_s	μ_d	Percent Increase $\frac{\mu_d - \mu_s}{\mu_s} \times 100$
Plain Steel	60-80	0.50	0.64	26
Plain Smooth Mortar	20-30	0.59	0.67	20
Plain Rough Mortar	20-30	0.74	0.82	---*
Teflon Coated Smooth Mortar	20-30	0.33	0.58	76
Teflon Coated Steel	20-30	0.33	0.56	70
Graphite Coated Smooth Mortar	20-30	0.32	0.44	38

* $\tan \phi = 0.84$

SECTION VI

CONCLUSIONS

The following conclusions are based on laboratory tests in which the coefficient of friction between drained sands and steel, cement mortar, Teflon, and graphite surfaces was measured at contact pressures up to 10 psig. and for loading times to initiate slip of 5 minutes and about one millisecond:

1. The static coefficients of friction are markedly affected by the size, angularity, and surface texture of the sand grains, regardless of the nature of the surface against which slip is occurring.
2. When the sliding surface is rough in comparison to the grain size of the sand, the angle of wall friction exceeds the angle of shearing resistance of the sand and sand/sand slip occurs. Since the angle of shearing resistance, ϕ' , of drained sands is practically uninfluenced by the rate of loading, $\tan \phi'$ is an upper limiting value for the coefficient of wall friction regardless of the rate at which slip is initiated.
3. In the case of unlubricated surfaces, the dynamic coefficient of friction is about 25 percent greater than the static coefficient, unless the conditions for sand/sand slip are approached.
4. At slow rates of loading, graphite is an excellent lubricant for both steel and mortar surfaces; Teflon was effective in the case of mortar surfaces but increased friction slightly in the case of the smooth steel surface.

5. At high rates of loading, both Teflon and graphite act as lubricants when compared to the plain surfaces; however, Teflon is less effective than graphite due, perhaps, to viscosity effects.
6. Once slip is initiated, the dynamic coefficient of friction increases slightly with increasing velocity (about 10 percent for velocities up to 30 inches/sec).

REFERENCES

1. Gaffey, J. T., 1964, "Development of Apparatus for Determination of the Dynamic Coefficients of Friction for Mortar/Sand Interfaces," Ph.D. thesis, Purdue University, Lafayette, Indiana.
2. Brumund, W. F., 1965, "Static and Dynamic Coefficients of Friction Between Sand and Selected Construction Materials," M.S.C.E. thesis, Purdue University, Lafayette, Indiana.
3. Leonards, G. A., 1963, "Laboratory Experiments on the Response of Soils to Shock Loadings," Technical Documentary Report No. AFSWC-TDR-62-90.
4. Kennedy, D. J. L., 1961, "A Study of the Failure of Liners for Oil Wells Associated with Compaction of Producing Strata," Ph.D. thesis, Graduate College University of Illinois, Urbana, Illinois.
5. Suklje, L. and Brodnik, J., 1963, "Deformation Conditions of the Mobilization of the Friction between Concrete and Soil," Acta Geotechnica 4-6, Ljubljana, Yugoslavia.
6. Potyondy, J. G., 1961, "Skin Friction Between Various Soils and Construction Materials," Geotechnique, Vol. XI, Number 4, Institution of Civil Engineers, London.

APPENDIX A

DETERMINATION OF THE FORCING FUNCTION

The shock tube used to produce the forcing function had a 4.5-foot rarefaction chamber and a 4.0-foot compression chamber with an inside diameter of 2.75 inches. Details of the relatively inexpensive shock tube that was constructed may be found in Reference 3.

Two methods were used to evaluate the forcing function. First, piezoelectric gages were placed on a rigid piston positioned in the downstream end of the shock tube. The average recorded pressure times the area of the piston was taken as the magnitude of the forcing function, which is shown plotted in Figure 2. By placing piezoelectric gages in the sidewalls of the shock tube, the shock wave velocity and the overpressure were measured directly, which permitted comparing of the theoretical reflected pressure on the piston with that actually recorded (1). The theoretical pressure acting on the fixed piston was about 7-10 percent greater than the pressure actually recorded by the gages. Part of this difference can be attributed to leakage around the piston face.

The forcing function, $F(t)$, having been determined, as described above, a moveable piston was placed in the downstream end of the shock tube. By measuring the velocity of this system with the LVDT, a set of time-displacement curves was obtained, which are compared with those obtained by double integration of $F(t) = m dv/dt$ in Figure 28. It is evident that excellent agreement was obtained.

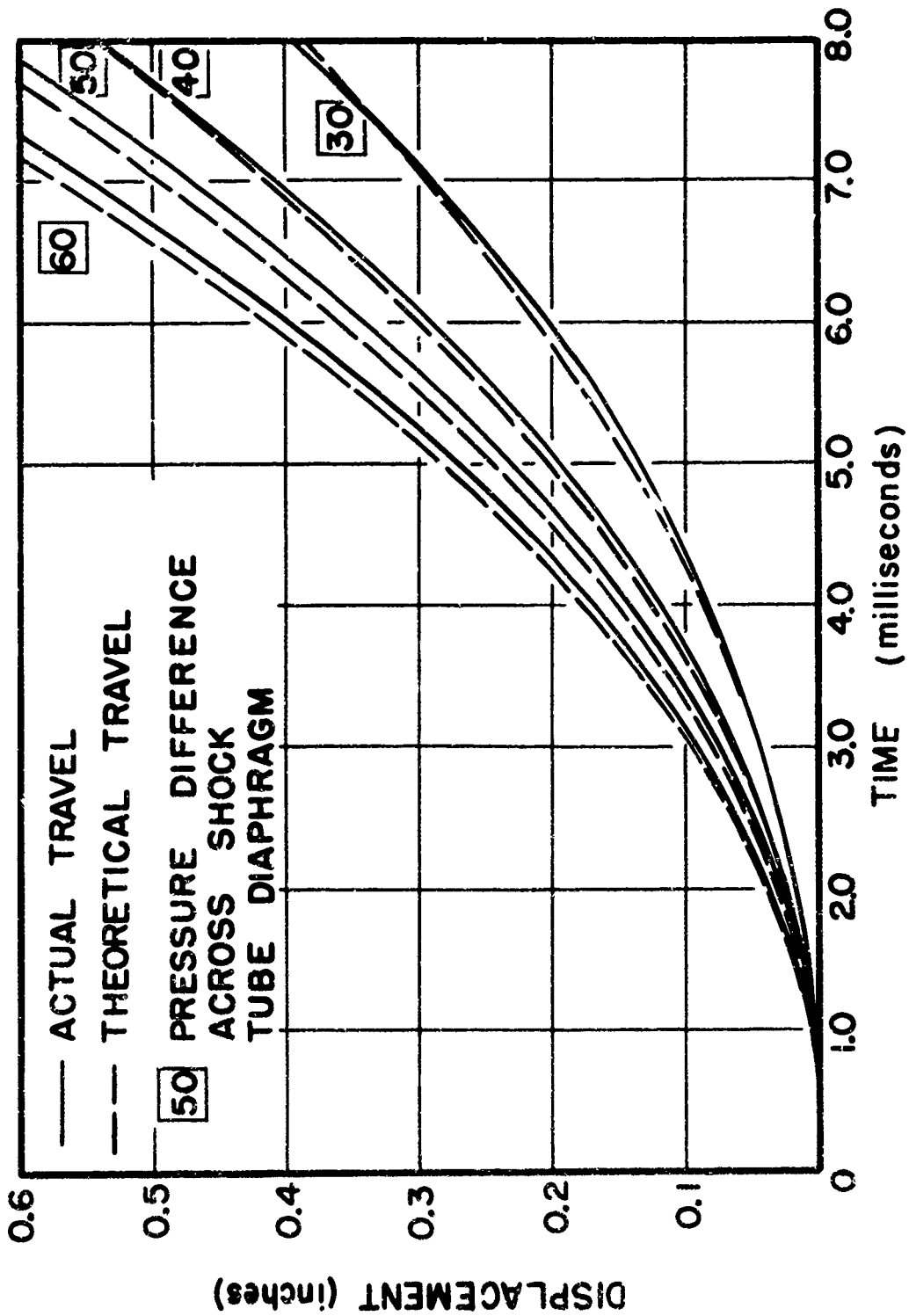


FIG. 28 VERIFICATION CURVES FOR F(1)

APPENDIX B

USE OF LINEAR VARIABLE DIFFERENTIAL TRANSFORMER FOR VELOCITY MEASUREMENTS

A Schaevitz No. 1000SL LVDT, consisting of a hollow cylindrical nonconductive coil form about $5/8$ inch in diameter was used. Three independent equally spaced coils are wound on the coil form. The center coil is the primary winding and the two flanking coils are secondaries. The transformer is provided with a cylindrical shield, fitting tightly around the coils, for both physical protection and electrostatic shielding from random electrical radiations. Inside the hollow coil form is a coaxial steel core about $1/4$ inch in diameter.

If direct current is fed to the primary coil, the core is converted into a magnet, setting up a flux field around it. If the core is moved, the flux field moves through the secondary coils, inducing a direct current voltage whose magnitude is proportional to the speed of the core, and whose phase is determined by the direction of motion of the core. If the secondary coils are connected in "series adding," the output voltages are amplified. The circuit needed to use the 1000SL LVDT as a velometer is shown in Figure 29.

To calibrate the LVDT, the core was connected to a piston in the shock tube and displaced a known distance (about 0.2 inches) from the end plate by means of a micrometer. A shock wave was generated in the tube and the output from the LVDT was recorded through the oscilloscope. A typical record is shown in Figure 30. The area under this curve equals the known initial displacement, whence a calibration factor of 258 inches/second-volt was obtained when the primary coil current

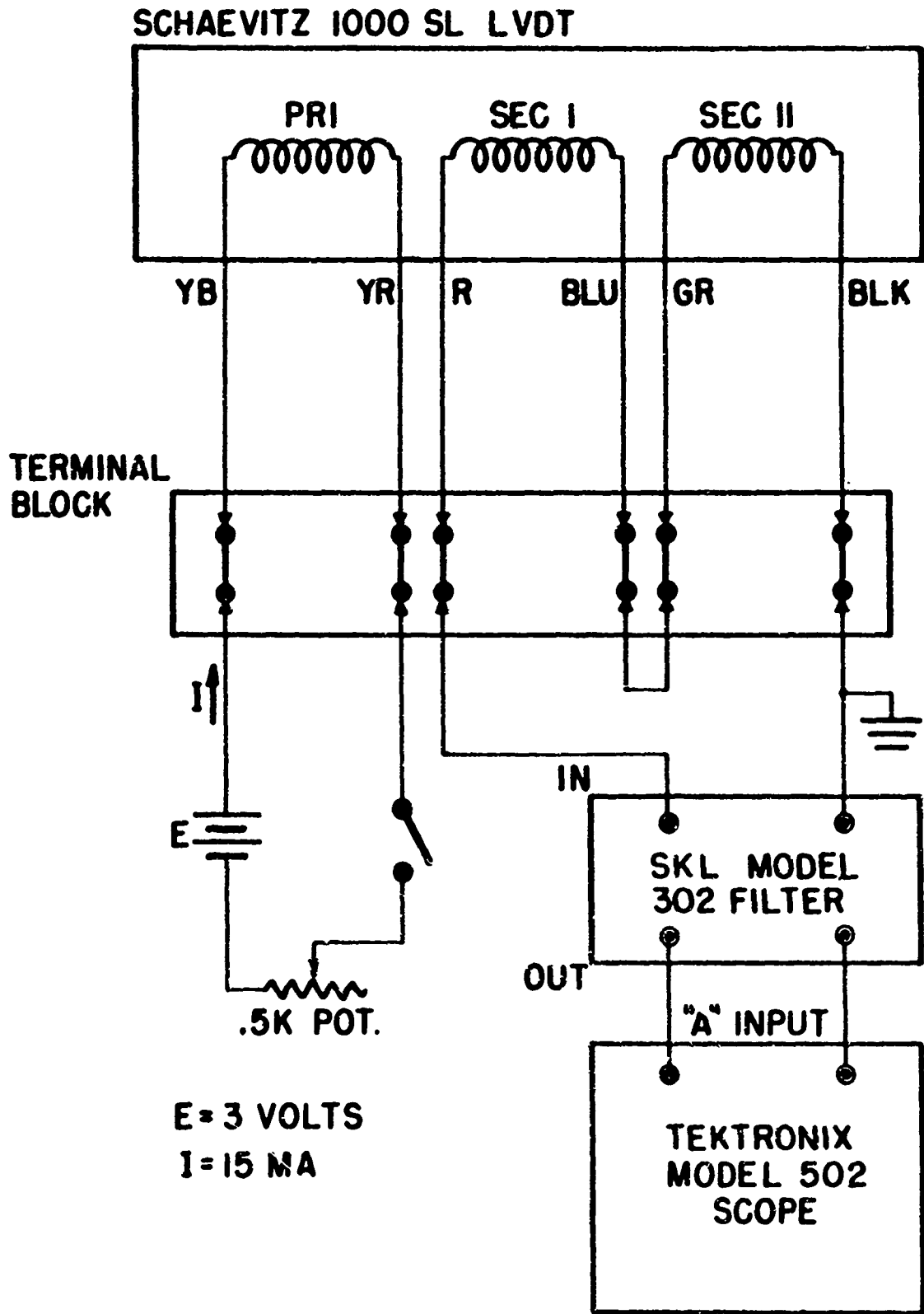


**FIG. 29 CIRCUI T DIAGRAM FOR LVDT USED AS
A VELOCITY TRANSDUCER**

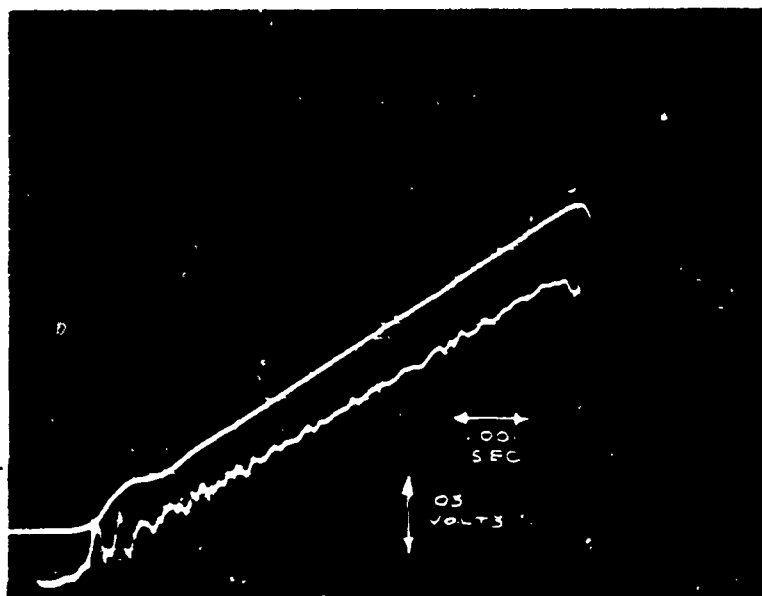


FIG. 30. TYPICAL TRACE FOR VELOMETER CALIBRATION

was 15 milliamps. The procedure was repeated with a variety of dummy loads added to the piston. In this manner the LVDT coil was moved over the range in velocities that developed in the dynamic friction tests without significant variation in the calibration factor.

APPENDIX C
SAMPLE CALCULATIONS

Static Tests

In the static test, the applied load minus the force needed to overcome the restriction of the rubber membrane at each end of the sample equaled the effective static friction force. By placing the rod in a sleeve to isolate it from the surrounding sand, the restraining force due to the membrane was measured and found to equal 9 pounds.

The confining pressures reported are nominal gage pressures. It was found that the vacuum gage was not accurate, and a calibration, using a mercury manometer, was performed (Figure 31). All computations used corrected gage pressures.

Sample Calculation:

Referring to Figure 24, for 20-30 sand on Teflon coated steel (static test No. 15),

$$\sigma_m = 5 \text{ psi gage}$$

Applied force - 79 lbs. (Virgin Pull)

The lateral area of the square steel rod is:

$$A = 4 \times 1 \frac{1}{8} \times 10 = 45 \text{ square inches.}$$

$$\text{Therefore, } \mu_s = \frac{F_s}{N_s} = \frac{F-9}{A \times \sigma_m \text{ actual}}$$

$$\mu_s = \frac{79 - 9}{45 \times 4.75} = \frac{70}{214} = 0.33$$

This result may also be found in Table V.

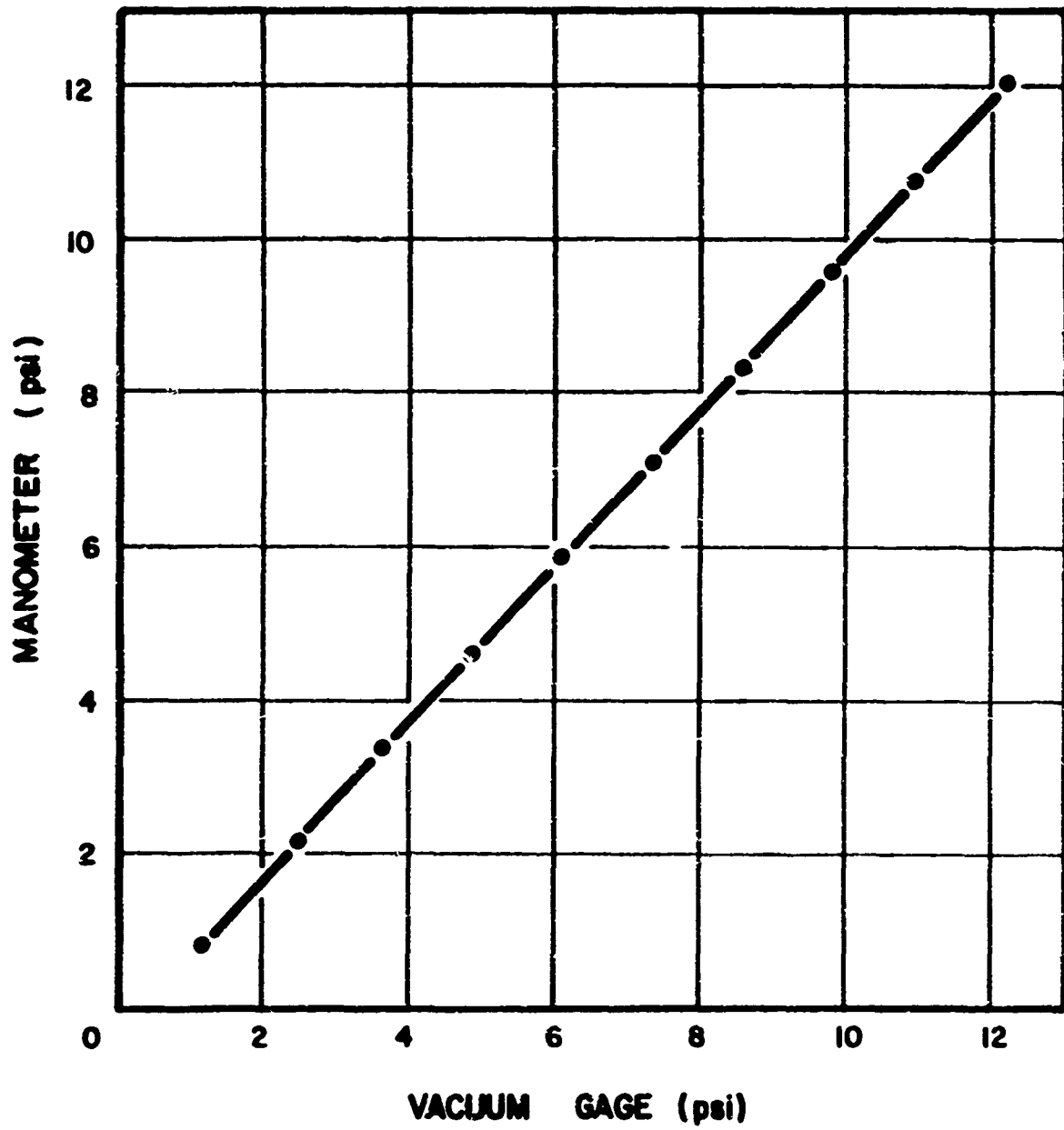


FIG. 31 VACUUM GAGE CALIBRATION

Dynamic Tests

For 60-80 sand on plain steel (dynamic test No. 2000 R)

1. Membrane pressure = $\sigma_m = 5$ psi gage

Therefore, $N_s = 214$ pounds

2. Forcing function (shock tube pressure = 40 psig).

From Fig. 2, $F(t) = 185$ pounds at 2 milliseconds (since $F(t)$ can be determined with an accuracy of ± 5 pounds, no attempt was made to correct for the restrictive effect of the membrane).

3. Mass of moving system

$$m = 1.43 \times 10^{-2} \frac{\text{lbs.} \cdot \text{sec}^2}{\text{in.}}$$

4. LVDT constant

$$258 \frac{\text{in}}{\text{sec-volt}} \text{ at 15 milliamperes through primary coil}$$

Sample Calculation:

Interpreting the LVDT trace shown in Figure 25,

sweep = 0.002 seconds/centimeter

sensitivity (top) = 0.02 volts/centimeter

slope of trace after slip:

$$\frac{2.4 \text{ cm} \times \frac{0.02 \text{ volts}}{\text{cm}}}{2 \text{ cm} \times \frac{0.002 \text{ sec.}}{\text{cm}}} = 12 \frac{\text{volts}}{\text{sec}}$$

The acceleration is:

$$12 \frac{\text{volts}}{\text{sec}} \times 258 \frac{\text{in}}{\text{sec-volt}} = 3.1 \times 10^3 \text{ in/sec}^2$$

$$\begin{aligned}
 \text{Therefore, } \mu_d &= \frac{F(t) - ma}{N_s} \\
 &= \frac{185 - (1.43 \times 10^{-2}) (3.1 \times 10^3)}{284} \\
 &= 0.66
 \end{aligned}$$

This result may also be found in Table VIII.

DOCUMENT CONTROL DATA - R&D		
<i>(Security classification of title, body of abstract and indexing annotation must be entered when the overall report is classified)</i>		
1 ORIGINATING ACTIVITY (Corporate author) Purdue University School of Civil Engineering Lafayette, Indiana		2a. REPORT SECURITY CLASSIFICATION UNCLASSIFIED
		2b. GROUP
3 REPORT TITLE EXPERIMENTAL STUDY OF STATIC AND DYNAMIC FRICTION BETWEEN SOIL AND TYPICAL CONSTRUCTION MATERIALS		
4. DESCRIPTIVE NOTES (Type of report and inclusive dates) 1 April 1962-1 April 1965		
5. AUTHOR(S) (Last name, first name, initial) Leonards, G. A.		
6. REPORT DATE December 1965	7a. TOTAL NO. OF PAGES 76	7b. NO. OF REFS 6
8a. CONTRACT OR GRANT NO. AF 29(601)-5204	9a. ORIGINATOR'S REPORT NUMBER(S) AFWL-TR-65-161	
b. PROJECT NO. 5710		
c. Subtask No. 13.144	9b. OTHER REPORT NO(S) (Any other numbers that may be assigned this report)	
d.		
10. AVAILABILITY/LIMITATION NOTICES Distribution of this document is unlimited.		
11 SUPPLEMENTARY NOTES	12. SPONSORING MILITARY ACTIVITY AFWL (WLDC) Kirtland AFB. NM 87117	
13. ABSTRACT A report is made of research carried out at Purdue University to determine, on the basis of laboratory measurements, the coefficient of friction between two sands of different gradation (one with angular and the other with rounded particles) in contact with Portland cement mortar, steel, teflon, and graphite. In the static tests, loads were applied at a uniform rate until slip occurred in approximately 5 minutes. Dynamic loads were applied by means of a shock tube, which produced a step-like forcing function; slip usually occurred in approximately 2 milliseconds or less. It was found that the coefficients of friction depend on the relative size, shape and surface roughness of the sand grains with respect to that of the surface in question; when the sliding surface is "rough" in comparison with the sand particles, the coefficient of friction approaches the coefficient of internal friction of the sand. Both graphite and teflon serve as friction reducers, compared to the plain surfaces, irrespective of the rate at which slip is initiated. For plain steel or cement mortar, the dynamic coefficient of friction was greater than the static coefficient of friction by about 25 percent, unless the static coefficient was such that sand/sand slip was approached. The angle of shearing resistance of the sand thus provides an upper limit to the coefficient of wall friction at all rates of loading.		

14 KEY WORDS Dynamic Soil Friction Dynamic Soil Response Soil Mechanics Friction Foundation Engineering	LINK A		LINK B		LINK C	
	ROLE	WT	ROLE	WT	ROLE	WT

INSTRUCTIONS

1. **ORIGINATING ACTIVITY:** Enter the name and address of the contractor, subcontractor, grantee, Department of Defense activity or other organization (*corporate author*) issuing the report.
- 2a. **REPORT SECURITY CLASSIFICATION:** Enter the overall security classification of the report. Indicate whether "Restricted Data" is included. Marking is to be in accordance with appropriate security regulations.
- 2b. **GROUP:** Automatic downgrading is specified in DoD Directive 5200.10 and Armed Forces Industrial Manual. Enter the group number. Also, when applicable, show that optional markings have been used for Group 3 and Group 4 as authorized.
3. **REPORT TITLE:** Enter the complete report title in all capital letters. Titles in all cases should be unclassified. If a meaningful title cannot be selected without classification, show title classification in all capitals in parenthesis immediately following the title.
4. **DESCRIPTIVE NOTES:** If appropriate, enter the type of report, e.g., interim, progress, summary, annual, or final. Give the inclusive dates when a specific reporting period is covered.
5. **AUTHOR(S):** Enter the name(s) of author(s) as shown on or in the report. Enter last name, first name, middle initial. If military, show rank and branch of service. The name of the principal author is an absolute minimum requirement.
6. **REPORT DATE:** Enter the date of the report as day, month, year; or month, year. If more than one date appears on the report, use date of publication.
- 7a. **TOTAL NUMBER OF PAGES:** The total page count should follow normal pagination procedures, i.e., enter the number of pages containing information.
- 7b. **NUMBER OF REFERENCES:** Enter the total number of references cited in the report.
- 8a. **CONTRACT OR GRANT NUMBER:** If appropriate, enter the applicable number of the contract or grant under which the report was written.
- 8b, 8c, & 8d. **PROJECT NUMBER:** Enter the appropriate military department identification, such as project number, subproject number, system numbers, task number, etc.
- 9a. **ORIGINATOR'S REPORT NUMBER(S):** Enter the official report number by which the document will be identified and controlled by the originating activity. This number must be unique to this report.
- 9b. **OTHER REPORT NUMBER(S):** If the report has been assigned any other report numbers (*either by the originator or by the sponsor*), also enter this number(s).
10. **AVAILABILITY/LIMITATION NOTICES:** Enter any limitations on further dissemination of the report, other than those

imposed by security classification, using standard statements such as:

- (1) "Qualified requesters may obtain copies of this report from DDC."
- (2) "Foreign announcement and dissemination of this report by DDC is not authorized."
- (3) "U. S. Government agencies may obtain copies of this report directly from DDC. Other qualified DDC users shall request through _____."
- (4) "U. S. military agencies may obtain copies of this report directly from DDC. Other qualified users shall request through _____."
- (5) "All distribution of this report is controlled. Qualified DDC users shall request through _____."

If the report has been furnished to the Office of Technical Services, Department of Commerce, for sale to the public, indicate this fact and enter the price, if known.

11. **SUPPLEMENTARY NOTES:** Use for additional explanatory notes.
12. **SPONSORING MILITARY ACTIVITY:** Enter the name of the departmental project office or laboratory sponsoring (*paying for*) the research and development. Include address.
13. **ABSTRACT:** Enter an abstract giving a brief and factual summary of the document indicative of the report, even though it may also appear elsewhere in the body of the technical report. If additional space is required, a continuation sheet shall be attached.

It is highly desirable that the abstract of classified reports be unclassified. Each paragraph of the abstract shall end with an indication of the military security classification of the information in the paragraph, represented as (TS), (S), (C), or (U)

There is no limitation on the length of the abstract. However, the suggested length is from 150 to 225 words.

14. **KEY WORDS:** Key words are technically meaningful terms or short phrases that characterize a report and may be used as index entries for cataloging the report. Key words must be selected so that no security classification is required. Identifiers, such as equipment model designation, trade name, military project code name, geographic location, may be used as key words but will be followed by an indication of technical context. The assignment of links, rules, and weights is optional.